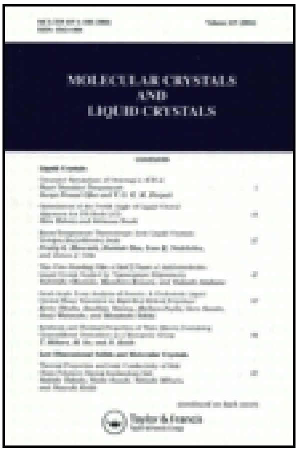

Molecular Crystals and Liquid Crystals
Publication details, including instructions for authors and subscription information:
http://www.tandfonline.com/loi/gmcl20

Linear and Non-Linear Polar Effects in Liquid Crystals

Sven T. Lagerwall [a]
[a] Chalmers University of Technology, Göteborg, Sweden

Version of record first published: 14 Jun 2011

To cite this article: Sven T. Lagerwall (2011): Linear and Non-Linear Polar Effects in Liquid Crystals, Molecular Crystals and Liquid Crystals, 543:1, 3/[769]-47/[813]

To link to this article: http://dx.doi.org/10.1080/15421406.2011.568326

Mol. Cryst. Liq. Cryst., Vol. 543: pp. 3/[769]–47/[813], 2011

ISSN: 1542-1406 print/1563-5287 online
DOI: 10.1080/15421406.2011.568326

Linear and Non-Linear Polar Effects in Liquid Crystals

SVEN T. LAGERWALL

Chalmers University of Technology, Göteborg, Sweden

In cholesterics and chiral smectics there are linear electro-optic modes of considerable interest. As they are fast-switching and have a natural gray scale we will discuss their future potential, in general for active matrix addressing. In spite of differences in physical origin they are all dielectric effects (even in the smectic C phase) and are generically related by symmetry. This leads to the common feature that there is only one time constant involved (not one "ON" and another "OFF" as for effects related to dielectric anisotropy). Furthermore this time constant is independent on the applied electric field. We will also see that cholesterics and chiral smectics have more in common – but seldom pointed out – than just being chiral.*

In surface-stabilized tilted chiral smectics there are instead strongly non-linear effects one of which may achieve a more or less perfect memory (bistability). If, in addition, the liquid crystal is polymer-stabilized, the cell can be made monostable with a continuous gray scale. As the effects are very fast they were originally successfully developed for passive matrix addressing. Industrial interest in these modes (ferroelectric and antiferroelectric) declined, nevertheless, in the late 1990s. This was not because other types of liquid crystals had been discovered but rather because a cost-effective thin-film-transistor (TFT) technology had been developed. With a TFT matrix every liquid crystal pixel is addressed individually and needs neither to have memory nor to switch at higher speed than can be achieved with nematics. As, however, active-matrix addressing is now commonplace there is naturally a renewed interest in these modes, especially for the future transfer from displays with color filters to displays in which the full color is generated by modulating the red, green and blue LEDs in the time domain.

1. Introduction

The aim with this review is to give the background for and to assess some of the fast electro-optic effects that could be considered as candidates to follow after the nematic effects already in use in high resolution LCDs. We have seen a tremendous development of nematic technology in the last decades, made possible first of all by the active addressing and by the dedicated efforts of the chemical industry to provide continuously optimized materials for the different effects. The active addressing by a matrix of thin-film transistors (TFTs) was pioneered by Peter Brody, then at Westinghouse in the USA in the 1970s and developed to maturity in Japan in the 1980s [1]. It has revolutionized the whole field of information displays such that even

---

Address correspondence to Sven T. Lagerwall, Chalmers University of Technology, S-412 96 Göteborg, Sweden. E-mail: sven.lagerwall@mac.com

small LCDs are almost unthinkable without TFTs. They have also permitted the OLEDs to be used in a display mode and led to a revival of an old LC mode. In fact, the Vertically Aligned Nematic (VAN) mode – now the leading technology in LCD TVs - was investigated already around 1970 at AEG-Telefunken in Germany (called DAP effect at that time) [2] but could not really be exploited before the advent of the TFT. The more recent In-Plane Switching (IPS) mode likewise could not work without TFT addressing.

While the Twisted Nematic (TN) was the first useful display mode, the originally used Mauguin version (achromatic regime) has since long disappeared and TN displays in first or second minimum (or maximum) mode are more and more being replaced by VAN and IPS displays. On the other hand, the big display manufacturers are investigating new liquid crystal materials that are intrinsically faster than nematics. An example of this is the recent interest in the blue phase Kerr effect mode that has a lot of attractive properties even if it requires high driving voltages.

Given the excellent quality of the latest large-screen TVs one might be surprised about this interest. There are several considerations behind it. One of them is that, even with 200 Hz update frequency, motion blur and color break-up cannot be completely avoided (the old CRT is here much better). Therefore some manufacturers aim at an update frequency as high as 500–600 Hz. Moreover, the recent 3D trend requires either to double the update rate or to effectively halve the number of lines in the display. The strongest argument is, however, that the color in all these TVs is still generated by an array of red-green-blue color filters. It is first of all very expensive, further it absorbs two thirds of the useful light. In order to show how incredibly energy-inefficient today's LCD TVs are we can start from the white LED backlight. First of all 50% of its light is, in principle, lost in the polarizers. (With new techniques one tries to recover part of this light.) Of the half that is left 70% is lost in the color filters. Then there is a 25% loss in the pixel aperture blocked by the TFT. Finally, you have to create the image (the picture cannot be just white), which gives an average loss of 85%. All this means that only about 1–2% of the backlight is actually transmitted. And it also means that these TVs draw *more* power, not less, than the old CRTs that they were made to replace.

There is of course a high priority to increase the energy efficiency of the LCD TVs. The single most important step towards this is to suppress the color filter array and generate the color in the time domain. The images for red, green and blue are then produced on the screen after each other under synchronous illumination of red, green and blue light from a LED array. This has to be done rapidly enough such that the frames merge in the human eye into the full color picture. This method is called Field-Sequential Color (FSC) and is already widely used in microdisplays. Obviously, FSC gives the further benefit of increasing the spatial resolution by a factor of three for a given size of display or, alternatively, reducing the number of transistors by a factor of three for a given number of pixels. It gives full color in each pixel without subpixellation but requires three times higher subframe rate. Thus this method requires an intrinsically very fast liquid crystal. One may increase the switching speed of a nematic by increasing the voltage or reducing the cell gap, but there is a limit in both. When reducing the cell gap the birefringence of the nematic has to increase in order to preserve the lambda-half condition in the white state, otherwise there would be a loss in transmission that we cannot afford. But the birefringence of nematics has been increased in the last decade to such levels that any further increase now seems unlikely.

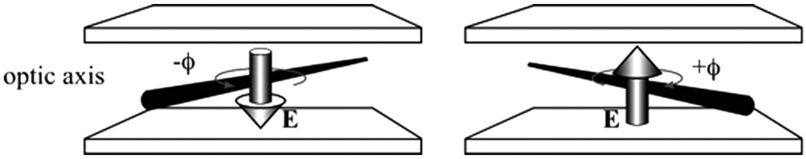

Figure 1. If a deflection ϕ of the optic axis is caused by an applied field **E**, with $\phi \sim E$, then we have a linear electro-optic effect. Three important effects belong to this category and are generically related. They are fundamentally different from the common effects using the dielectric anisotropy in liquid crystals.

This motivates the present interest in other, faster, LCD modes. Besides the blue phase mode, which will not be discussed here, these can be found in cholesterics and chiral smectics. Below we will focus on three linear and three non-linear modes and discuss their good and bad points.

2. Linear Modes

These modes are unique because they are not only dielectric and analog but they are symmetric in their response to the electric field. The modes are generically related and can all be described by the illustration of Figure 1.

The electric field is applied in the usual way between the two glass plates confining the liquid crystal. The response is a deflection of the optic axis by an angle ϕ. The effect is linear and symmetric in the sense that if we reverse the sign of the field, $E \rightarrow -E$, then also the sign of the deflection is reversed, $\phi \rightarrow -\phi$. Thus, ϕ can only be a function of odd powers of E,

$$\phi = a \cdot E + bE^3 + \ldots \tag{1}$$

and, keeping only the first term, we simply write

$$\phi \sim E \tag{2}$$

The three modes of this character are the flexoelectro-optic mode in cholesterics, the electroclinic effect in smectic A* and the deformed-helix mode in smectic C*. These three electro-optic modes have in common that the response ϕ is linear in E. The effect is a pure dielectric response, the induced polarization P_i being proportional to E. It is thus not related to dielectric anisotropy. In each case the deflection ϕ involves a rotation of the optical indicatrix which is simultaneously transformed from uniaxial to biaxial. A further characteristic distinguishing them from conventional liquid crystal modes is that there is only one time constant τ – no τ_{ON} and τ_{OFF}. Finally, the response time τ does *not* depend on the applied field. All these properties – strictly valid in the low-field limit – are a consequence of the symmetry that these phenomena have in common.

The basic thing was already stated in Eq. (2), that the induced tilt is proportional to the field. Writing this in vector form

$$\vec{\phi} = a \cdot \vec{E} \tag{3}$$

we notice that $\vec{\phi}$ is an axial vector while $\vec{E}$ is a polar vector and a a material parameter. Hence, in order for the left hand and right hand side to have the same symmetry (to transform in the same way) the material parameter a has to be a pseudoscalar. Hence the medium must be chiral. This means that the effect exists in SmA* (the electroclinic effect) but not in SmA, in N* (the flexoelectro-optic effect) but not in N, in SmC* (the deformed-helix mode) but not in SmC. It does not mean that the coupling to the electric field is chiral, but the medium must be chiral. Nobody is surprized that the cholesteric is considered to be chiral or that SmC* is chiral. But it is strange that there is still the incredibly common (and serious) misconception that SmA* – which shows the electroclinic effect – is not chiral, i.e., that the medium is non-chiral as long as the field has not interacted. But the electric field $\boldsymbol{E}$ is not chiral (has symmetry $C_{\infty v}$) and cannot induce chirality, formalized in Curie's principle [9]. Sometimes people claim that SmA and SmA* have the same symmetry because they superficially "look" the same. But this is no more trivial than that a sugar solution in water that turns the plane of polarization of light looks the same as a (non-chiral) water solution that does not. The symmetry difference not only means that the electroclinic effect is absent in SmA but also, for instance, that a SmA* phase is harder to align in bookshelf geometry than a SmA phase. SmA and SmA* interact differently with a substrate. It is also incorrect (senseless) to write a phase transition sequence (as very often done)

$$Iso - SmA - SmC^*$$

because a phase transition SmA – SmC* does not exist. Another way to look at this is to consider that certain orthogonal smectics in which the material has a very high intrinsic twisting power may have a transition to a TGB phase

$$SmA^* - TGB,$$

where a helix only shows up in the TGB phase although it is evident that also the first phase must be chiral. To use the Curie principle once more: a phase transition, i.e., a transition under a change in a scalar parameter, the temperature T, (non-chiral) cannot change the reflection properties of the material. Therefore one should be careful to distinguish non-chiral SmA and chiral SmA* even if none exhibits a helix. Likewise a SmC* where the helix is unwound or non-existent for other reasons (surface-stabilized) is still a SmC*, not a SmC. The chirality does not vanish because the helix vanishes. We have to care about this in order to avoid inconsistencies.

Although none of the flexoelectro-optic, electroclinic or deformed helix modes have been successfully commercialized so far, they have each an interesting potential. But each has also problems.

2.1. *The Flexoelectro-Optic Effect*

In the flexoelectro-optic effect an electric field E, applied perpendicular to the helix axis of a short-pitch cholesteric makes the director turn an angle $\phi(E)$, as shown in Figure 2. The optic axis is perpendicular to the director, hence the optic axis turns by the same amount. The pitch of the cholesteric has to be smaller than the wavelength of light and the helical axis, which is the optic axis, has to be parallel to the glass

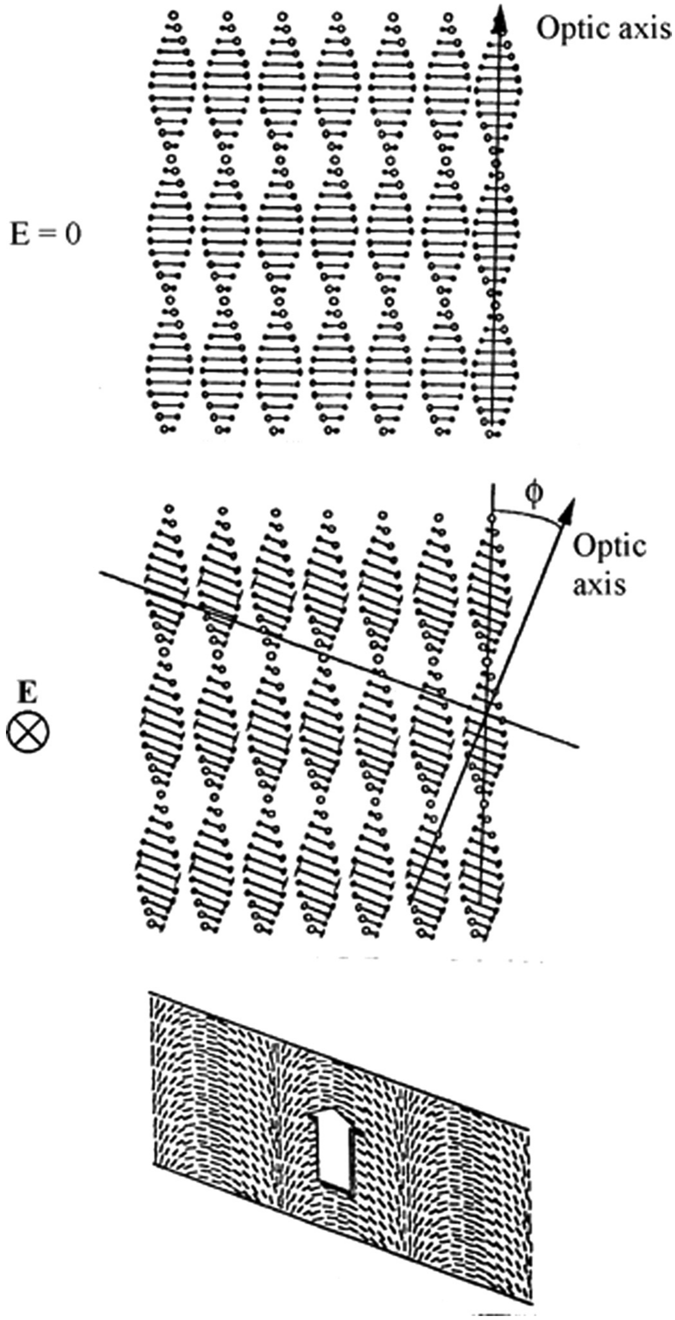

Figure 2. The deviation of the optic axis in a (hardtwisted, $p < \lambda$) cholesteric when an electric field **E** is applied perpendicular to the axis of continuous symmetry. The cholesteric geometry allows a flexoelectric polarization to be induced in the direction of **E**. A plane along the field containing the directors cut out of the middle figure (thus perpendicular to the paper) is shown below, illustrating the splay-bend and its inherent polarization (From [8]).

plates (a tricky texture). The deviation $\phi(E)$ is linear in E up to tilts of more than 30° with response times in the range 20 μs to 100 μs. Because of the linearity, if we reverse the sign of E the optic axis deviates in the opposite direction, $-\phi$. Finally, $\phi(E)$ is practically independent of temperature, which is a fairly unique property for a liquid crystal effect. This powerful electrooptic effect was introduced by Patel and Meyer in 1987 [3] and studied by them in the following years [4,5]. In the decade that followed it was further developed mainly by Rudquist [6–8].

What happens physically is that the electric field E induces a polarization P proportional to E (dielectric effect). This polarization is generated in form of a periodic splay-bend deformation in the director field, which is a polarized state. It appears in any plane cut perpendicular to the new optic axis. Splay and bend deformations are coupled to a local polarization of the liquid crystal via the flexoelectric effect. The field-induced deviation of the optic axis is thus an inverse flexoelectric effect. Further illustrations of the sometimes intricate geometry involved in the effect can be found in the work referred to, but in particular in [8] and [9].

When discussing this device it is useful – as well as in many other contexts – to keep the old word *cholesteric* to represent the very tightly twisted form of the species, as distinguished from *chiral nematic* that signifies the only weakly twisted form. The two are physically quite different: the first is optically uniaxial negative, the second positive; the first has a different elasticity that gives a tendency for focal conic structures; the second is easy to align, the first is difficult to align other than planar (Grandjean).

In order to give a feeling for the characteristics of this electro-optic effect we will briefly sketch a derivation of the dynamical properties. In presence of an electric field E the free energy density is written

$$f = \frac{1}{2}K_{11}(\nabla\cdot\mathbf{n})^2 + \frac{1}{2}K_{22}(\mathbf{n}\cdot\nabla\times\mathbf{n})^2 + \frac{1}{2}K_{33}(\mathbf{n}\times\nabla\times\mathbf{n})^2 - \mathbf{E}\cdot\mathbf{P} \tag{4}$$

where the K_{ii} are the Oseen constants and

$$\mathbf{P} = e_s\mathbf{n}(\nabla\cdot\mathbf{n}) + e_b(\mathbf{n}\times\nabla\times\mathbf{n}) \tag{5}$$

We have here neglected the dielectric term since it is quadratic in the field and also since we require $\Delta\varepsilon$ to be very small. We start out with the helix axis along the z direction, then $\mathbf{n} = \cos kz$, $\sin kz$, 0) where k is the cholesteric wave vector. If we now apply the field in the y direction, $\mathbf{n}$ changes to $\mathbf{n} = (\cos kz\ \cos\phi,\ \sin kz,\ -\cos kz\ \sin\phi)$ which we insert in (4). After putting the average values of $\sin^2 kz$ and $\cos^2 kz$ equal to 1/2 we find for the total free energy

$$f = \frac{1}{4}(K_{11}+K_{33})k^2\sin^2\phi + \frac{1}{2}K_{22}k^2(1-\cos\phi)^2 - \frac{1}{2}(e_s+e_b)Ek\sin\phi \tag{6}$$

Taking $\partial f/\partial\phi = 0$ we finally find the value of tilt that minimizes the free energy. The result is, using the abbreviations $1/2(K_{11}+K_{33}) = K$ and $1/2(e_s+e_b) = e$,

$$\tan\phi = \frac{eE}{K_{22}k} + (1 - K/K_{22})\sin\phi \tag{7}$$

For moderate deflection angles we put $\tan\phi \approx \sin\phi$, and we find that, in this limit, the dependence on the twist vanishes,

$$\tan\phi = \frac{eE}{Kk} \tag{8}$$

The twist constant K_{22} does not appear in this simple expression. To first order the deformation takes place at constant helical pitch ($k = \text{const}$). There is no unwinding in the field and therefore no hysteretic effects. In the small angle limit (8) further reduces to

$$\phi = \frac{eE}{Kk} \quad \text{or } \phi = a \cdot E \tag{9}$$

The pseudoscalar property of a lies in the dependence on k.

In the same limit the free energy expression (6) reduces to

$$f = \frac{1}{2}Kk^2\phi^2 - eEk\phi \tag{10}$$

The Landau-Khalatnikov equation in irreversible thermodynamics tells us that after a perturbation in a variable (in this case ϕ) it relaxes back with a speed that is proportional to the rate of change of the free energy with respect to this variable, with a kinetic coefficient having the dimension of an inversed viscosity

$$\frac{\partial\phi}{\partial t} = -\gamma^{-1}\frac{\partial f}{\partial\phi} \tag{11}$$

From (10) this gives

$$\gamma\frac{\partial\phi}{\partial t} = -Kk^2\phi + eEk \tag{12}$$

This can be recognized as a Debye equation

$$\gamma\frac{\partial\phi}{\partial t} + A\phi = BE \tag{13}$$

often written, by introducing a characteristic time $\tau = \gamma/a$,

$$\tau\frac{\partial\phi}{\partial t} + \phi = (B/A)E = \frac{e}{Kk}E \tag{14}$$

The saturated value of induced tilt ($\partial\phi/\partial t = 0$) is found to $\phi_s = (b/a) = eE/Kk$ in conformity with (9). The induced tilt as a function of time is given by the solution of (14)

$$\phi(t) = \phi_s(1 - e^{-t/\tau}) \tag{15}$$

with

$$\tau = \frac{\gamma}{Kk^2} \tag{16}$$

When the field is taken away the induced tilt relaxes back to zero with the same characteristic time

$$\phi(t) = \phi_s e^{-t/\tau} \tag{17}$$

The flexoelectric coupling is not chiral, so what is then the role of chirality in this case? The answer is that the helically twisted state is the only one that is flexoelectrically "neutral" (there is no local polarization related to twist) and therefore the only state from where a splay-bend deformation can grow continuously from zero in a symmetric fashion independent of the direction of E. How it grows is illustrated in Figure 3.

To summarize: for small deflections the optic axis is switched out an angle ϕ proportional to E

$$\phi = \frac{eE}{kK} \tag{9}$$

where e is the average of the splay and bend flexoelectric coefficients, K the average of the splay and bend elastic constants (K_{11}, K_{33}), and k the helical wave vector. As we see the deflection is counteracted by the splay-bend elasticity (K) and is also

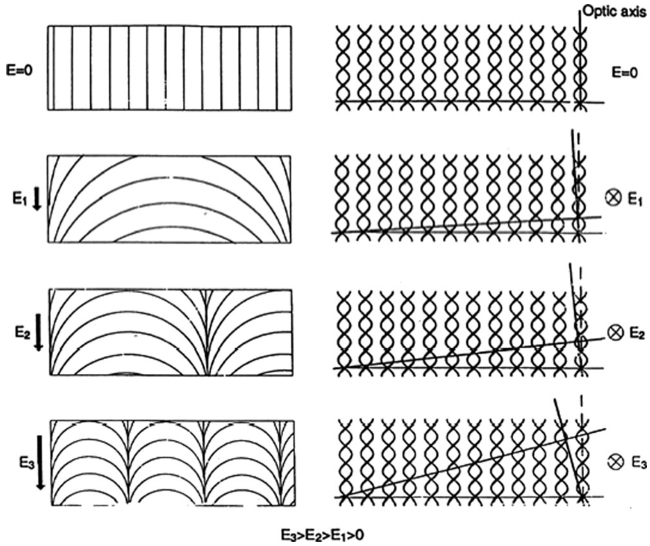

Figure 3. Field-induced periodic splay-bend pattern (left) in the director field (in any oblique cut perpendicular to the optic axis) and optic axis deflection with increasing field (From [7]).

smaller the more hard-twisted (k) the cholesteric. The twist elastic constant K_{22} does not enter the problem for small ϕ: the deflection takes place at constant twist.

In the same approximation the switching time τ is given by

$$\tau = \frac{\gamma}{Kk^2} \tag{16}$$

where γ is the rotational viscosity. As we see, comparing with Eq. (9) there is a trade-off between maximum deflection for a certain field and the switching speed. Thus the value of k has to be optimized. An interesting feature of Eq. (9) is that for a cholesteric with a temperature-independent pitch, ϕ is temperature independent, because both e and K are proportional to S^2, where S is the nematic order parameter containing the temperature dependence. In Eq. (16) γ and K only partly compensate each other in this respect. As it is not difficult to make a cholesteric with constant k independent of temperature, we see that the flexoelectrooptic effect will have an induced tilt ϕ which is temperature independent and a dynamics which is weakly temperature dependent and, in addition, independent of the applied field. The latter is true because E does not exert any quadratic torque on the molecules as long as $\Delta\varepsilon \approx 0$. It only determines the equilibrium angle of ϕ.

Assessment. The flexoelectro-optic effect is an *in-plane switching* that should be ideal to combine with TFTs (in conventional electrode geometry, i.e., with the field applied across the cell gap) to produce a continuous gray scale. The cell gap does not have to be very thin, in fact, it must not be very thin (because the effective birefringence is low), which gives the drawback that the applied voltage is rather high. Switching times in the 20 μs–100 μs region were achieved by Rudquist but since then no essential progress in performance has been reported. Thus it would require some materials engineering to raise the value of e, which could nowadays perhaps be achieved by doping with bent-core molecules. Otherwise the chemistry required in order to optimize some material parameters (Δn, $\Delta\varepsilon$, k, e) seems relatively straightforward. The really vulnerable point is stable alignment. In the past a number of standard and non-standard methods have been tried to align the helix homogeneously along the glass plates with only modest success. Thus more than twenty years after the pioneering work no breakthrough in alignment procedures has been reported. There is first of all a strong tendency for the obtained texture to transform into the stable Grandjean texture with time. The goal must be to achieve the other structure without the need of applying any electric fields during the aligning process, i.e., only by action from the surface. Such a surface should have alternating stripes on a scale of about 0.3 μm or less promoting homeotropic and planar anchoring. It could possibly be photo-patterned on self-assembled monolayers (SAMs) by interference illumination of two UV laser beams. Once achieved it could be stabilized by a polymer network. But there are even more problems. These have to do with the fact that the cholesteric is not a conventional nematic but in its physical properties lies between nematic and smectic. Its smectic-like properties (the periodicity along one direction) tend to induce characteristic texture instabilities at high voltages, similar to those that we will encounter in the electro-optic mode to be described next.

2.2. *The Electroclinic or Soft-Mode Effect*

When we approach the critical temperature T_c from above for the phase transition $SmA \rightarrow SmC$, the elastic constant that keeps the director orthogonal to the layer weakens. At T_c it becomes zero and the tilt becomes spontaneous, cf. Figure 4. Near T_c the tilt fluctuations are very large, and *if the system is chiral* we can, due to the coupling between θ and P, induce a tilt above T_c by applying an electric field perpendicular to the layer normal. This soft mode is called the electroclinic effect. It was

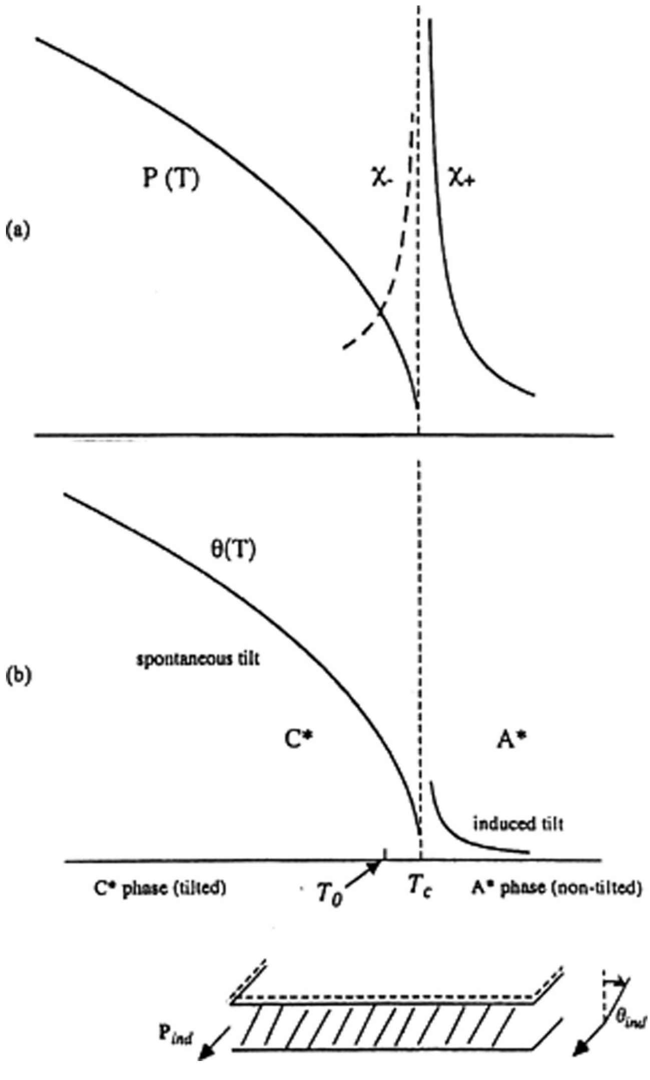

Figure 4. Growth of spontaneous polarization $P(T)$ related to the tilt θ below the tilting transition in a typical SmA*-SmC* material (a). In (b) is shown the electrically induced tilt above the tilting transition. At the bottom is illustrated how one single smectic layer shrinks when the originally upright molecules tilt. P, θ and the layer shrinkage δd are all coupled to each other. The susceptibility χ (for P as well as for θ) follows the same functionality on either side of T_c but is twice as large above T_c.

likewise predicted by R.B. Meyer who investigated it together with his student S. Garoff [10]. The tilt direction is reversed if we reverse the direction of the electric field. To make a useful electro-optic effect the smectic A* layers have to be uniformly stacked perpendicular to the glass plates (so-called bookshelf geometry). We thus again have a field-sensitive optic axis (the director) swinging out in a plane parallel to the glass plates (*in-plane switching*) and perpendicular to the applied field. The induced tilt is small and to first order proportional to the field.

In the *non-chiral* case, the SmA-SmC transition, which is typically of second order, is described by the simple Landau expansion in free energy

$$f = \frac{1}{2}a\theta^2 + \frac{1}{4}b\theta^4 + \dots \tag{18}$$

with $a = \alpha(T - T_c)$. The free energy is the same for $+\theta$ as for $-\theta$, because it cannot depend on which way the director tilts away relative to the smectic layer normal. Therefore no odd powers can appear in (18), which leads to the well-known parabolic growth of θ below the Curie point. If we now make the material chiral the transition SmA*-SmC* will happen at almost the same temperature and the tilt θ will grow in the same parabolic way. However, in this chiral case the appearance of non-zero tilt θ will be accompanied by the appearance of a non-zero polarization P. While P has little effect on the transition as such, it contributes to the free energy, not only electrically but also entropically, because polar order means additional order and carries an entropic cost. The corresponding Landau expansion therefore has the form, valid on both sides of the transition,

$$f = \frac{1}{2}a\theta^2 + \frac{1}{2\varepsilon}P^2 - cP\theta - PE \tag{19}$$

where we have skipped the term to fourth order in θ as we want to study the region close to, but in particular, just *above* the Curie point, where θ certainly is small. Instead we have added the contribution from an external electric field E.

In this expansion θ is the primary order parameter and P, which depends on θ, is a secondary order parameter. The third term expresses the coupling between θ and P. The expansion (19) is valid in absence of helix (as in the surface-stabilized state, see below).

We have to minimize f with respect to both θ and P. Starting with the latter, $\partial f/\partial P = 0$ gives

$$P = \varepsilon c\theta + \varepsilon E \tag{20}$$

If there is no electric field we see that

$$P = \varepsilon c\theta \tag{21}$$

i.e., the polarization is proportional to the tilt in the C* phase where $\theta \neq 0$. With respect to θ we further get

$$\frac{\partial f}{\partial \theta} = a\theta - cP = 0 \tag{22}$$

or, with Eq. (20) inserted,

$$a\theta = \varepsilon c^2\theta + \varepsilon cE \tag{23}$$

and finally

$$\theta = \frac{\varepsilon cE}{a - \varepsilon c^2} = \frac{\varepsilon cE}{\alpha(T - T_c)} \tag{24}$$

by way of writing the equality

$$a - \varepsilon c^2 = \alpha(T - T_0) - \varepsilon c^2 = \alpha(T - T_c) \tag{25}$$

Here $T_c = T_o + \varepsilon c^2/\alpha$ is the renormalized transition temperature. The transition has been shifted to slightly higher temperature in the chiral material.

We may now write the relation between induced tilt and applied field simply as

$$\theta = e_c(T) \cdot E \tag{26}$$

where e_c is the electroclinic coefficient. As we see, this coefficient is strongly dependent on temperature,

$$e_c = \frac{\varepsilon c}{\alpha(T - T_c)} \tag{27}$$

The electroclinic effect has a certain similarity to the converse piezoelectric effect: when the molecules tilt the layer shrinks, cf. bottom of Figure 4. Thus the field induces a strain. This strain is, however, electrostrictive ($\sim E^2$) and there is no converse to the electroclinic effect. The *SmA** phase is thus not piezoelectric. But if it would be polymerized into a soft (rubber-like) solid, this solid would be piezoelectric.

In principle the electroclinic effect exists on either side of T_c, but the induced tilt is smaller (half the value) and also harder to detect below T_c in the presence of the larger spontaneous tilt. Essentially, therefore, the electroclinic effect is the field-induced tilt of the director in the SmA* phase or, by extension, in any chiral orthogonal smectic.

As already stressed SmA and SmA* do not have the same symmetry. Their symmetry difference not only means that the electroclinic effect is absent in SmA but also, for instance, that a SmA* phase is harder to align in bookshelf geometry than a SmA phase. As any surface adjacent to a liquid crystal generally has polar properties, it acts like a field and induces a tilt, which can be looked upon as a surface electroclinic effect. This means that a bookshelf-aligned SmA* actually has a biaxial SmC* structure adjacent to a surface, a considerable practical alignment complication which is absent in the non-chiral SmA phase.

Let us now turn to the dynamics. The Landau-Khalatnikov Eq. (11), here written

$$-\gamma\frac{\partial\theta}{\partial t} = \frac{\partial f}{\partial\theta} \tag{28}$$

with the right hand side taken from (22) leads to

$$-\gamma\frac{\partial\theta}{\partial t} = (a - \varepsilon c^2)\theta - \varepsilon c E \tag{29}$$

Again, we see that this is a Debye equation like (13)

$$\gamma\frac{\partial\theta}{\partial t} + A\theta = BE \tag{30}$$

with $A = \mathrm{a} - \varepsilon c^2 = \alpha(T - T_\mathrm{c})$. It can also be written in the convenient form

$$\tau\frac{\partial\theta}{\partial t} + \theta = e_c \cdot E \tag{31}$$

with emphasis on the two controlling electro-optic parameters

$$e_c = \frac{\varepsilon c}{\alpha(T - T_c)} \tag{27}$$

$$\tau = \frac{\gamma}{\alpha(T - T_c)} \tag{32}$$

Thereby we have finally brought the problem back to the already studied case of the flexoelectro-optic effect. The difference between these two equations and the corresponding Eqs. (14) and (16) is that in this case we have a very strong temperature dependence. Otherwise the physics is the same. We also note from Eq. (32) that also here the switching time does not depend on the applied field. If we look at the bottom of Figure 4 we see why: the field does not exert any torque on p_{ind}. This is valid as long as we can ignore the quadratic dielectric effect. If the reader is still puzzled by the fact that the switching time does not depend on E it might be helpful to point out that this does not mean that the momentaneous angular speed of the director should be independent of E. That τ does not depend on E means – here as well as for the flexoelectro-optic effect – that the time it takes for the optic axes to swing out to a certain fraction of the saturation value is independent of E. But because that value is proportional to E the same is valid for the angular velocity of the director.

In Figure 4 the induced tilt is exaggerated. Practically it can often be about 10° but in most materials only a couple of degrees. On the other hand, when the tilt is small, the electroclinic effect is ultrafast (sub-microsecond response). In the last decade electroclinic materials have been synthesized with large tilt, especially by the groups at the Naval Research Labs [11] and in Boulder, recently even of up to 25° (with a correspondingly slower response, in the 10 to 100 microsecond regime) [12]. It is clear from Eq. (24) that if we approach the tilt transition very large tilts can be induced at the same time as the electro-optic response slows down. On the other hand, when we approach $\mathrm{T_c}$ the electroclinic effect gets non-linear for large applied fields and Eq. (26) is no longer valid. At the same time as the response time τ gets shorter the induced tilt shows a tendency for saturation with the asymptotic behavior $\theta \sim E^{1/3}$ [36]. But it is of course very inconvenient to work in this regime.

As just mentioned, different efforts have been made to increase the tilt. In reality the electroclinic effect was for a long time a pre-transitional curiosity (although of high academic interest) with measured deflection angles of a fraction of a degree before it was demonstrated [13] that this angle could be increased by orders of magnitude in the so-called bookshelf configuration. This is the geometry with the layers stacked perpendicular to the glass plates used in experiments on surface-stabilized smectic C*. In fact, several groups, when measuring the polarization as a function of temperature in the C* phase, had found a small tail on the other side of the C*–A* transition without realizing that its origin is the electroclinic effect.

The long synthetic efforts during the last decades have not only been directed towards increasing the tilt and possibly reducing the temperature dependence but also to solve a different nasty problem connected with the fact that the electroclinic effect is markedly *electrostrictive*, which means that when the director tilts, the layer shrinks. At large applied fields, i.e., at large induced tilts, this leads to a kind of layer buckling instability creating ripples parallel to the layer normal that compromise the electro-optic effect. This problem – together with the chevron problem of the same origin in chiral smectic displays – has given rise to a new sub-area of research with the goal of producing new materials, commonly called *de Vries smectics*, that do not show any layer shrinkage at the tilting transition SmA-SmC. The simplest model of such a smectic is an A*-C* material in which the molecules are already tilted in the A* phase (essentially with a tilt equal to the saturated tilt in the C* phase) but with tilt directions that are completely disordered such that the optic axis averages out to be along the layer normal. The transition A* → C* in this model is therefore an *ordering* transition [14] taking place without changing the layer thickness. At T_c the molecules just start to order in tilt direction and, as the temperature is further reduced, the apparent tilt grows and finally approaches the molecular tilt. One would expect that the electroclinic effect in the A* phase of such a material would take place without layer shrinkage.

A few compounds that more or less seem to approximate this behavior had been synthesized in 1989 but their importance for devices and display technology was not recognized until a decade later. Now more and more of them are being found. Recently David Walba and his coworkers at the University of Colorado in Boulder have created new such smectics that represent a very important step towards ideal electroclinic materials. One key feature of these materials is that they have a SmA-SmC transition that is *weakly first order*.

The electroclinic response in one of these materials, W415, on both sides of the tilting transition is shown in Figure 5. First of all it can be seen that the induced tilt is very high at quite moderate applied fields. Second, the temperature dependence of the tilt shows a completely new behavior in the A* phase. At low fields the λ-shape can still be recognized as we cross T_c but at higher field the shape changes from concave to convex making the temperature dependence far less dramatic. To explain this we can go to the classic study of how a chiral smectic with a first order tilting transition behaves in the presence of an external field, as reported by Bahr and Heppke in 1987 [15]. As recognized by Jacques Prost the transition has a certain similarity to the liquid-gas transition in the neighborhood of the critical point, cf. Figure 6. At zero field θ falls off in a parabolic-like way in the C* phase as we increase the temperature, except that, at the transition temperature T_o, there is a discontinuity (in reality this is very small since we are dealing with very small tilt) where θ drops directly to zero. If we apply a field, θ increases in the C* phase but twice as much in the A*

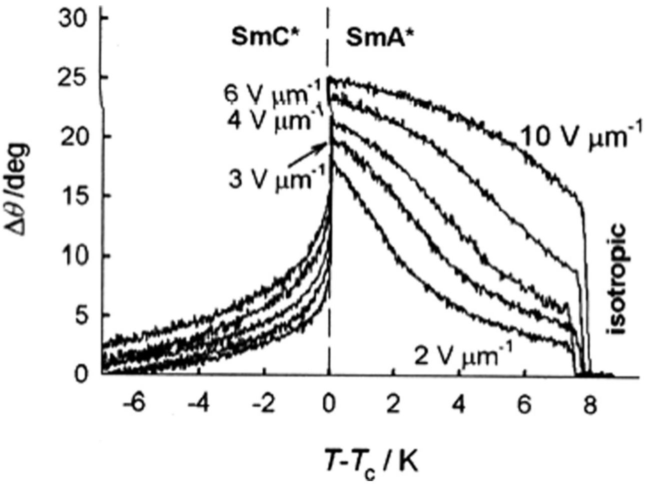

Figure 5. Electroclinic effect on both sides of the tilting transition in the compound W 415. (From reference 12.).

phase, therefore the discontinuity decreases at the same time as θ grows continually in the A* phase. But with higher field we have to raise the temperature in order to bring about the transition to the lower-tilted phase, hence T_o increases. Finally, at a critical field E_c, corresponding to a critical temperature T_c, the two phases merge to be the same thing. Above (T_c, E_c) the two phases have the same symmetry and we can move from one to the other in a continuous way – there is no phase transition.

The unwanted problematic behavior of e_c and τ expressed in Eqs. (27) and (32) is a characteristic feature of a second order phase transition. In such a transition, as we approach T_c fluctuations will grow out of order and cause different material parameters to behave in a singular way. If, however, the transition is first order, even weakly, we do not come as close to this critical region and already at small applied

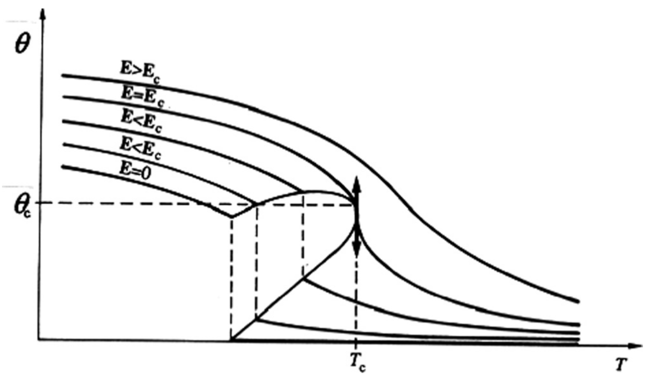

Figure 6. Tilt as a function of temperature and applied electric field in a compound having a first order A*-C* transition. Above the critical point (T_c, E_c) we can move from very high to very small tilt but there is no change in symmetry. Only below the critical point there is a phase transition. (From reference 16.).

fields the moderate fluctuations will be quenched and the undesired singular behavior at least greatly modified as can be seen in Figure 5. As expected W 415 also shows a very small layer shrinkage. Perhaps it is soon time [17] for applying the electroclinic effect?

Assessment. The electroclinic effect in the A* phase is, in principle, the fastest useful liquid crystal electro-optic effect, but its use will be limited mainly due to the strong temperature dependence, which would require cells with temperature stabilization. At the present stage it seems rather suitable for modulators than displays. Nevertheless, with more than 20° tilt achievable in W 415 (at such high tilts the switching speed is somewhat lower) and its moderate *T*-dependence in such materials it would be interesting to investigate the electroclinic effect in reflective mode on a silicon backplane. It may of course find use in other applications. One of the most interesting is chirality sensing. If we dope a non-chiral smectic A with a chiral compound its electroclinic response will be proportional to the enantiomeric excess, which can therefore be measured. It turns out that this effect has the potential to give the most sensitive detector of chirality that has been found so far [18].

2.3. *The Deformed Helix Mode*

This electro-optic effect, (DHM), is the response of a tightly twisted helical SmC* aligned with the layers perpendicular to the glass plates and with a uniform layer orientation. It was invented by the Moscow group and reported in 1980 [19]. Unlike the two previously described linear modes it has been the subject of a considerable industrial effort, a collaboration in the 1990s between Philips in Holland and Roche (later Rolic) in Switzerland. If the helical pitch is smaller than the wavelength of the light than the SmC* is optically uniaxial with the optic axis along the layer normal. In Figure 7 the projection of the helix is shown to the upper left and the corresponding optical indicatrix to the right.

When a field is applied the helix is deformed as the first stage of a process (middle part of the figure) that later will lead to a complete unwinding of the helix at higher fields. This gives an averaged tilt of the optic axis $\langle\theta\rangle$, which for small values of E is proportional to E. It is illustrated in the figure as the inclination of the indicatrix by the angle $\langle\theta\rangle$. We then again have a field-controlled optic axis. As the indicatrix also changes shape, the effective birefringence increases, just as in the electroclinic case.

The physics involved is here the unwinding of the helix in the C* phase by an external electric field. This is a dielectric process that takes place without threshold. A field $\pm E$ induces a polarization $\pm\langle P\rangle$ that initially grows from zero as, $\langle P\rangle \sim E$ and, when the unwinding is complete, has attained its full value P, the spontaneous polarization (ignoring the small electroclinic contribution). At this point $\langle\theta\rangle$ is of course equal to the full value θ. The smectic C* phase is helielectric, and this unwinding has certain similarities to a paraelectric response: the gradual turning of the present dipoles into the direction of an external field. The difference is that the dipoles in this case are ordered (this is the helielectric order) and not disordered.

The fact that the effective $\langle P\rangle$ changes when the optic axis swings out is a complicating factor in the electronic addressing of a display.

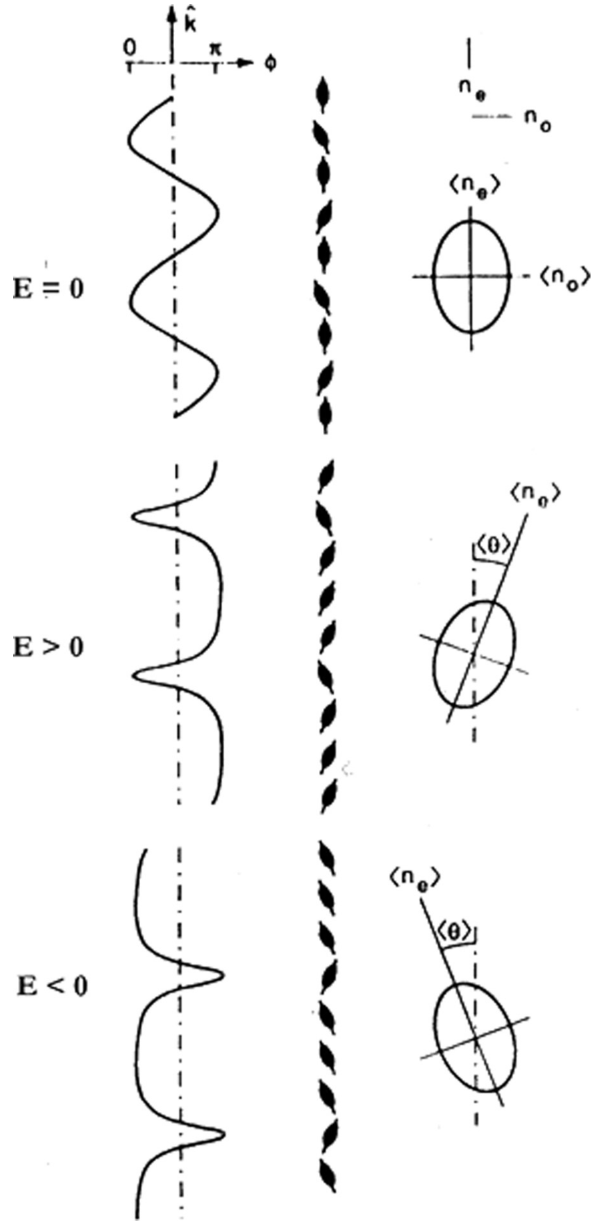

Figure 7. Partial untwisting of the SmC* helix in an electric field gives a linear electro-optic mode. The averaged tilt direction $\langle \theta \rangle$ in the presence of the field increases as a linear function of the field, $\langle \theta \rangle \sim E$. From [20].

To find the dynamics we equate the viscous torque to the sum of the ferroelectric and elastic torques and get (see, for instance [9]), neglecting the action from the surfaces,

$$\tau = \frac{\gamma}{PE + Kq^2} \tag{33}$$

For a hard-twisted smectic C* and moderate fields we may put $Kq^2 \gg PE$ and get

$$\tau = \frac{\gamma}{Kq^2} \tag{34}$$

which is very similar to (16) although γ and K do not mean exactly the same thing. Thus, for moderate fields, E does not enter the expression. A further similarity to the flexoelectro-optic case is that τ is practically independent on T, because γ and K both scale as $sin^2\theta(T)$. Hence the only dependence is in the helical pitch, which can be made fairly temperature independent. It turns out that also the switching times are quite comparable in the two cases.

The great advantage in the deformed helix mode would then lie in the possibility to achieve a very large tilt of the optic axis and also fulfill the $\lambda/2$ condition. Ideally the tilt could be as large as θ. With $\theta = 45°$ this would also be a perfect electro-optic mode. Smectics C are known with 45° tilt, moreover, in this case θ is normally independent on T. But these smectics have a direct N-C transition whereas a phase sequence N-A-C is required in order to achieve a reasonable alignment, already sufficiently complicated by the strong twist. In N-A-C materials the tilt can be as large as about 30°. In reality, however, an optic axis deflection of this order is impossible to attain because as soon as the helix not only get deformed, but untwisted, hysteretic effects appear that make the mode completely impractical as they lead to image retention effects ("sticking"). Therefore, the switching angle is very limited, to perhaps about 15°. It means that even in this respect the DHM is rather comparable to the flexoelectro-optic effect. One big advantage that the symmetric linear modes share is that the electronic addressing can – at least in principle – be very simple, though at the cost of losing a factor of two in speed. One just has to use two frames for every image, applying $+E$ in the first, $-E$ in the second frame, thus avoiding any DC effects. This presupposes of course that the mode is perfectly symmetrical, i.e., that the transmission $T(+E)$ is exactly the same as $T(-E)$. Otherwise the image will suffer in contrast. The writing speed must also be the same. But in one state the induced polarization points into, in the other state out of the confining surface. Therefore the surface alignment layers ought to be polar-neutral, which is almost impossible to realize, in particular for materials with high value of spontaneous polarization. But at least the over-all cell symmetry has to be polar-neutral. As we see, we have a number of additional complications in displays using polar materials. Nevertheless, matrix-addressed DHM display prototypes have been presented [21], demonstrating analog gray scale and video speed although with moderate performance. Due to alignment defects there is undesired transmission in the dark state and, in combination with the limited deflection angle, the contrast ratio is low, on the order of 50:1.

Assessment. The deformed helix mode has the very serious disadvantage of using a chiral medium with a very tight twist – a disadvantage it shares with the flexoelectro-optic effect. There just is no aligning surface adjusted to such a structure. In the DHM case additional problems exist from the polarity of the phase and, in particular, from the peculiar defects that appear in tilted smectics, defects that will be discussed in the following paragraphs. But of course the viewing angle is excellent as in all these modes. It is a pity that still no studies have been made of the flexoelectro-optic effect in active matrix drive. If one tried, the performance would probably be quite surprising.

If we compare the three linear modes discussed so far, the electroclinic or soft mode effect appears the most promising. This is first of all due to the fact that we can achieve an excellent (and stable) dark state with an orthogonal smectic whereas the other materials are notoriously difficult to align. Perhaps one could give them a new chance by using nanofabricated surfaces, considering the great progress in pre-programmed block-polymer self-assembly in recent years [37]. A less sophisticated way to apply the linear modes would be to skip the bookshelf geometry and align the layers (or phase levels in the cholesteric) parallel to the substrates, in combination with in-plane electrodes. Also here the SmA* would stand out giving the best darkstate. The geometry would exactly correspond to Garoff and Meyer's first experiments demonstrating the electroclinic effect. Because of its very high speed this mode really ought to be tried out with the best de Vries-like materials. Note its similarity to the VAN mode in nematics - but in this case the on- and off-switching are equally fast.

3. Non-Linear Modes

In the last section we discussed a dielectric mode in the prime example of a chiral tilted smectic, the C* phase. All chiral tilted smectics are very particular materials because they have vector properties. They have a spontaneous polarization that is a local polarization in every infinitesimal volume. As we already saw, this leads to an electro-optic effect that depends on the sign of the applied field. These facts were predicted by R.B. Meyer in 1974 and shortly after verified [22]. With $\boldsymbol{z}$ as the unit vector along the layer normal the polarization is given by

$$\boldsymbol{P} = P_o \boldsymbol{z} \times \boldsymbol{n} \tag{35}$$

In the non-tilted (SmA*) phase $\boldsymbol{z} \times \boldsymbol{n} = 0$ and $\boldsymbol{P} = 0$, but $\boldsymbol{P}$ increases as the tilt angle θ grows in the SmC* phase. The plus or minus sign indicates that $\boldsymbol{P}$ can be sterically connected to $\boldsymbol{n}$ in two possible ways. For instance, W46 (a Walba substance) has a polarization of $P = +45\,\mathrm{nC/cm^2}$ at $\theta = 31°$. This means that its opposite enantiomer (its mirror-image stereoisomer) by symmetry must have its polarization in the opposite direction, thus with negative sign. We also note from (35) that the spontaneous polarization has to be perpendicular to the director in order not to be in conflict with the director symmetry $\boldsymbol{n} = -\boldsymbol{n}$. For a polarization to exist the medium has to be chiral and the chirality manifests itself as a helical twist of the director with a period p typically in the μm range. Over this distance there is thus a self-cancellation of $\boldsymbol{P}$ in the volume. Except by an electric field we can act on the helical superstructure by adding a chiral dopant with an antagonistic twisting power and make the structure more weakly twisted, and in principle we could achieve a SmC* structure with $p = \infty$. This does not mean, however, that we would get a structure with a uniformly directed $\boldsymbol{P}$. The result is instead a complicated, partly self-cancelling splay-bend-twist structure that is completely non-useful [9].

As we saw in the last section, the smectic C* phase *per se* is not ferroelectric. Its symmetry, D_∞, does not allow ferroelectricity. But it may, together with the surfaces, form a structure that shows a non-linear typical ferroelectric response. This led to the first manufacture of bistable liquid crystal displays, demonstrating several attractive electro-optical properties like in-plane switching, wide viewing angle and high speed.

3.1. *The Surface-Stabilized State*

The existence of a polar vector $\boldsymbol{P}$ everywhere has a number of interesting but also complicating consequences. The main new feature is that an applied electric field $\boldsymbol{E}$ exerts a torque $\boldsymbol{P} \times \boldsymbol{E}$, trying to turn $\boldsymbol{P}$ into the direction of the field. This action is thus sensitive to the sign of the field, in contrast to other liquid crystal effects, which are based on the anisotropy of ε and quadratic in E ($\sim E^2$).

In the C* phase the electroclinic effect can be neglected, thus the torque by the field causes the connected ***P*-*n*** pair to move around the tilt cone at constant θ. If, as in the last section,we bring a helical SmC* into an electroded cell in such a way that the smectic layers are perpendicular to the cell plates ("bookshelf geometry") and apply a field across the cell we would start to wind up the helix shown in Figure 8 top. By inversing the field we make the director move on the cone from one side to the opposite one. The result is that the optic axis has been switched by an angle 2θ. This is shown in the figure where the surface condition is assumed, for simplicity, to require that ***n*** lies in the plane of the cell. If the field is reduced to zero, the structure resumes its helical state, having symmetry D_∞. This may take considerable time, even hours, but ultimately the helical ground state reappears. This is the effect that we already discussed in the previous section, except that there the helical pitch was smaller than the wavelength of light. Here, we will instead imagine that we have an N*-A*-C* material in which the helical pitch has been made large in both the N* phase (as the liquid crystal is aligned in this phase) and in the C* phase.

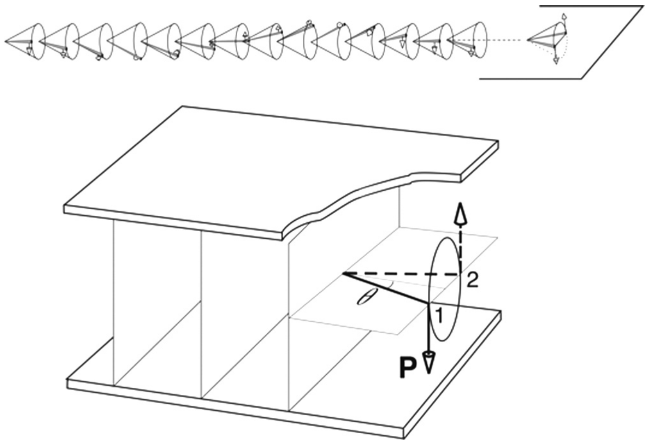

Figure 8. In the "Bookshelf geometry" the smectic layers stand upright, perpendicular to the surfaces like the books in a bookshelf. The helix axis is parallel to the glass plates. While a helical structure is well developed in the middle of a (reasonably thick) cell, especially if the pitch is much smaller than the cell gap, $p \ll d$, it is incompatible with the surface conditions, which take over when $p \geq d$. Thus, the helix is unwound in thin enough cells. The constraint that the director has to be on the cone and at the same time parallel to the surface (a different surface condition is also possible), selects just **two** possible director states, giving ferroelectric properties (SSFLC). From [40].

If we now reduce the cell thickness to a very small value, of the order of the helical pitch which is typically 1 to 2 micrometer for most single SmC* substances, something qualitatively different happens. Spontaneous domains appear side by side representing up and down state polarization, respectively. The reason for this is that the surface state is incompatible with the helical state which exists in the bulk, i.e., in the middle of the cell. This helical state has to be connected to the surface states by two near-boundary zones of periodic defects (disclinations). These zones represent a high elastic energy and invade proportionally more and more of the sample, the thinner the cell. Finally, the completely unwound state, i.e., the ***P*** up or ***P*** down state, has a lower energy than the state with a quasi-helix plus defects, and therefore is the equilibrium ground state. This phenomenon is called "surface-stabilization" [41]. The surface-stabilization transfers the local C_2 symmetry to the whole medium and any uncompensated helix with pitch larger than the cell gap is intrinsically absent. An applied electric field now switches UP domains into DOWN domains, or vice versa according to the sign of the field. Furthermore, both states are in principle (see below) symmetrically stable, hence remain when the field is taken off. We thus have a bistable device. In fact, the surface-stabilized structure has the typical properties of a solid ferroelectric. The response has the characteristic form of a ferroelectric hysteresis loop (Fig. 9) with distinct threshold and two oppositely polarized states at zero field.

This structure is therefore called a surface-stabilized ferroelectric liquid crystal (SSFLC). The smectic C* phase is only ferroelectric under *confinement*, and the appearance of ferroelectricity is probably the most dramatic effect of confinement known in liquid crystals. But as every SmC* material can be surface-stabilized, the shorter acronym FLC is commonly used. As a result of the surface-stabilization you get rid of the helix. You could also get rid of the helix by doping the SmC* with a convenient chiral material to make the pitch infinitely long ($p \to \infty$). But this does not give you any spontaneous domains. Thus surface-stabilization is not just a trick to get rid of the helix. It is a way to force the SmC* out of its natural crystallographic state, to a new symmetry that allows a macroscopic polarization.

What has been said so far about switching and bistability, however, corresponds to the conceptions that were predominating around 1980. Before we enter into the complications found as the work proceeded, let us look at the basic electro-optics corresponding to that simple picture.

3.2. *The Electro-Optics*

With one polarizer adjusted to the optic axis (1) in Figure 8 and the second polarizer crossed, (1) becomes the black state. If the switching angle 2θ equals 45°, and if the thickness of the cell corresponds to the $\lambda/2$ condition, the SSFLC in the switched state (2) changes the direction of vibration to be exactly in the transmitting direction of the second polarizer, as illustrated at the top of Figure 10. The optimum conditions giving 100% transmission in the bright state are thus that $\theta = 22.5^\circ$ together with $\Delta nd = \lambda/2$ or $\lambda/\Delta nd = 2$. In general the expression for the transmitted intensity (with 100% corresponding to the transmission through parallel polarizers) is given by

$$I = I_0 \sin^2 2\alpha \sin^2(\pi \Delta nd/\lambda) \tag{36}$$

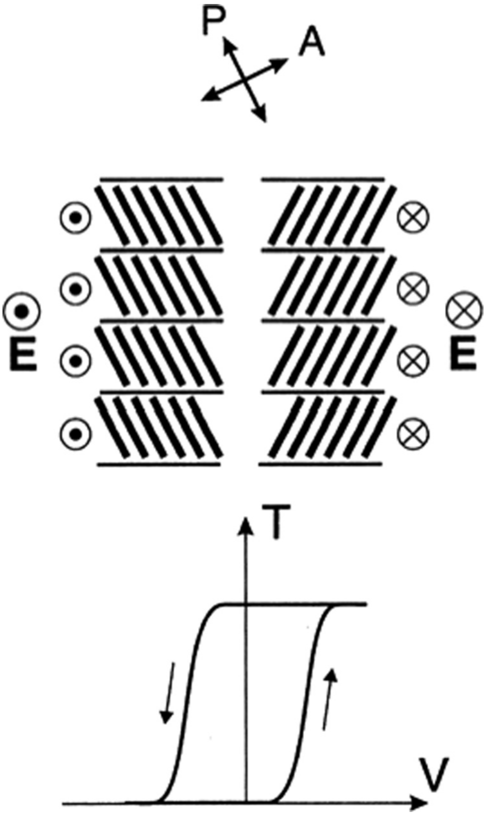

Figure 9. Ferroelectric switching in the chiral smectic C* phase. The molecules move on the surface of the smectic cone between two surface-stabilized states when the spontaneous polarization aligns along the applied field. The electro-optic response is a characteristic single hysteresis loop in the transmission *T*. The polarizer-analyzer setting, as indicated, makes the left state dark and the right state bright. From [40].

with the switching angle α in this case equal to the full cone angle 2θ. The second factor determines the transmission as a function of wavelength (color). For $\theta = 22.5^\circ$ this transmission is shown as a function of optical path in Figure 10. As we see, the SSFLC device has the advantage of being relatively achromatic if the half-wave condition is fulfilled in the middle of the visible spectrum. The fact that the optic axis in both states lies in the plane of the cell ("in-plane switching") furthermore gives a contrast with almost hemispherical viewing angle. An important feature of the SSFLC is that it is a binary device. The two states give no natural gray scale. The switching between the two states, on the other hand, is very fast, both ways. The response speed for the undisturbed motion around the cone is proportional to the torque $\boldsymbol{P} \times \boldsymbol{E}$ and inversely proportional to the counteracting rotational viscosity. The switching time is given by Eq. (33) where we can put $q \approx 0$, i.e., we have in FLC the case opposite to DHM, cf. Eq. (34). This gives a characteristic response time

$$\tau \approx \frac{\gamma}{PE} \tag{37}$$

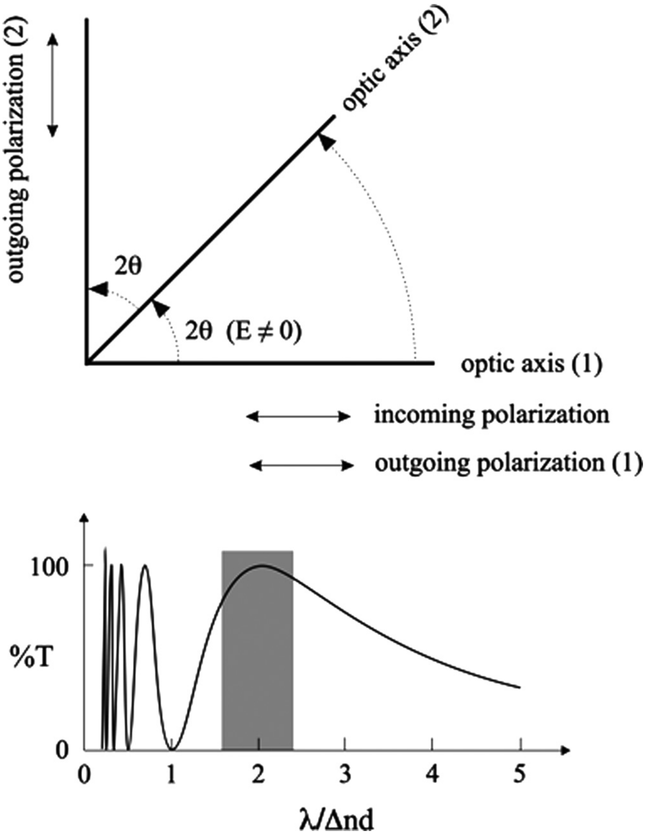

Figure 10. The ideal SSFLC cell is a switchable half-wave plate. For one sign of applied field, the slow axis (i.e., the director **n**) is in the same direction (1) as the first polarizer. By reversing the field, the slow axis (effective optic axis) is switched into the (2) direction at an angle 2θ from (1). The action of a $\lambda/2$ plate is to turn any polarization into its mirror state relative to the optic axis. Thus, if $2\theta = 45°$, the incoming polarization is turned into the orthogonal direction and is admitted by the analyzer. In the bottom drawing is shown the transmission for this case of $2\theta = 45°$. The range of visible light is indicated around the half-wave condition $\lambda/\Delta nd = 2$. From [40].

inversely proportional to the applied field. This is the characteristic time for the collective rotation of the director in the bulk of the sample and lies in the μs regime for typical fields. However, as the surface switching is responsible for the latching into the memorized state, it turns out that there is a threshold as a *voltage-time* area of the applied switching pulse. It is not a static voltage threshold as in a Frederiks transition in a nematic. Instead it is a dynamic threshold for a switching process counteracted by a viscous torque $\gamma\partial\phi/\partial t$. If we then allow twice as much time for the switching to be accomplished this torque would just be half as strong. Thus with a pulse width of 50 μs the threshold voltage for latching may be 8 volts while we have to go to 40 volts in order to switch with pulses of 10 μs duration. Line addressing times of the order of 10 μs are indeed possible for FLC devices, making them strongly competitive for television applications among passively addressed displays. On the other hand, with the advent of TFT technology allowing active addressing, pulse times of milliseconds are compatible with the required frame time. This means that FLC is also very well adapted for the combination FLC-TFT as here the threshold voltage goes down to the order of 1 V.

3.3. *The Less-Ideal Picture*

What has been summarized so far is a drastic oversimplification of the facts. Recognizing the future potential of FLC, there have been important industrial efforts. Thereby a number of serious problems have been found, making FLC (and AFLC, see below) the – beyond comparison – most complicated liquid crystal technology to date. Already working with a cell thickness of 1–2 μm in a large area display is a formidable manufacturing problem. The bistability itself is a tricky problem because its origin lies in surface action and *is not, as in solid ferroelectrics, a material property*. Achieving symmetric bistability is not a trivial challenge, not least while the boundary conditions tend to be polar rather than polarity-neutral. The hysteresis loop in Figure 9 is often asymmetrically displaced to the left or right. An interesting option is to deliberately displace it to the point that there is only one stable state for $E = 0$. Such a monostable device requires active addressing (TFT) but has a natural gray scale. In passive driving the gray scale otherwise has to be generated by temporal or spatial dither, or by a combination. This, together with the requirement of DC-compensated waveforms and the serious problem of "sticking" (memorized information which is not easily erasable – a well-known problem in all kinds of LCDs), make heavy demands on the electronic addressing techniques. In practice, sticking still limits the value of P that can be used in an FLC display (and thereby the speed according to Eq. (37). Nor can the applied field E be too high, with the same consequence, as at very high fields disruptive structural defects appear. One also has to pay attention to the addressing waveforms because DC, not AC, pulses must be used for writing the desired state. This will require inserting certain time slots just to achieve over-all AC balance (blanking). In addition, asymmetric waveforms (even when there is no DC component) may at high fields induce a form of layer instability known as field-induced layer rotation, which completely ruins the bookshelf structure, cf. Figure 11. Such instabilities appear in the non-tilted chiral phase (A^*) as well as in the tilted (C^*, C_a^*) [23]. They can be suppressed by polymer stabilization [24] but of course, better in the first place by a careful design of the electronic addressing waveform.

Even much more important is, however, that the bookshelf geometry is a highly idealized structure. In reality the layers are not perpendicular to the cell plates but slightly inclined or rather folded, making a so-called chevron structure [25]. The chevron by itself reduces the effective switching angle, as shown in Figure 12. Moreover, the fold can occur in two main directions, with or against the pretilt – C1 and C2 chevrons, respectively – and where C1 and C2 regions join so-called zigzag defect lines appear with a different contrast, cf. Figure 13. In order to avoid such defects, precautions have to be taken so that the whole display structure consists of entirely C1 or entirely C2. This may require a tilt angle θ considerably less than 22.5°, reducing the achievable contrast further.

Finally, electro-flow effects have to be avoided and a sophisticated spacer technology is required as any smectic structure with layers in a direction other than along the cell plane is mechanically fragile. In spite of all these difficulties, very powerful and interesting FLC devices and displays have been manufactured. (For a discussion

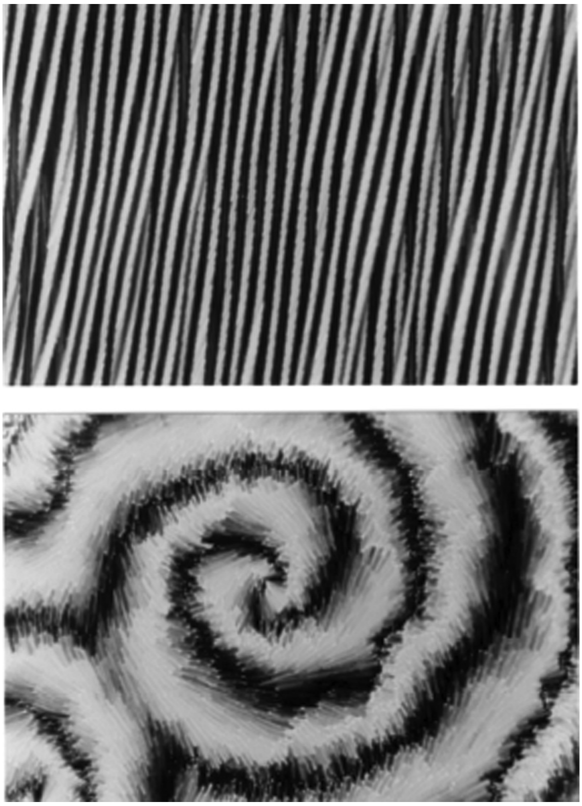

Figure 11. Field-induced rotational instability. When applying an alternating electric field with no DC component but with an asymmetric waveform to a smectic A* or C*, a continuous shift in the direction of the local layer normal may be induced. Angular velocities as high as 1°/sec may be set up by a simple sawtooth of 10–20 Hz and 50 V/μm. In the upper picture the beginning of layer destruction is seen, in the lower the chaotic texture that may be seen already after a couple of minutes. There is a threshold in the applied field which depends on material, surface treatment and shape of the applied waveform. The effect is generally more pronounced in smectic A* than in smectic C*.

of numerous early prototypes see, for instance, reference 9.) These FLC displays are the first examples of application of *smectic materials*.

3.4. *FLC Displays*

In the middle of the 1980s not only Japanese companies began to show interest in the FLC technology but also European groups such as Thorn EMI in Great Britain, Philips in Holland and the French LETI group in Grenoble. They were all pioneers in different ways. Thorn EMI were the first to propose color sequential backlighting, now normally called FSC (field sequential color), Philips were the first to demonstrate active matrix-controlled FLC gray scale by charge controlling the fraction of switched microscopic domains, and LETI had an entirely original and simple FLC technology combining temporal and spatial dither useful for moderate size video displays aiming at a different market than Canon. When the LETI group were

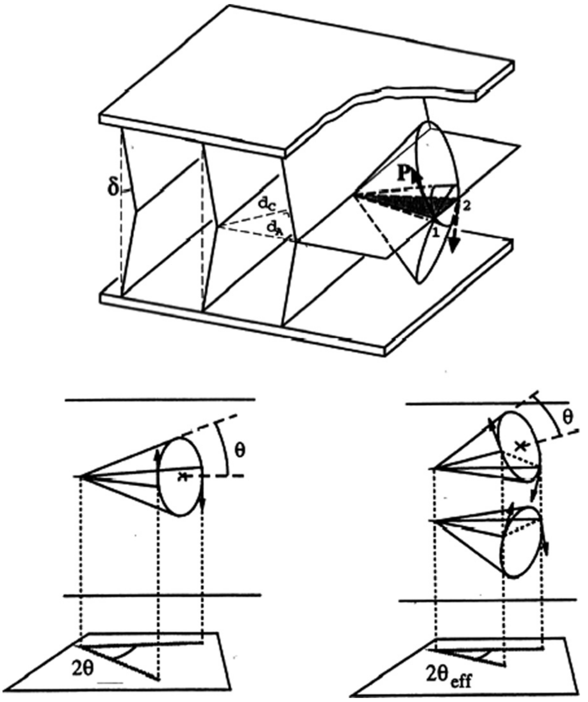

Figure 12. The shrinkage in smectic layer thickness due to the molecular tilt $\theta(T)$ in the SmC* phase results in a folding instability of the layer structure ("chevrons"). Even if the fold can be made to go everywhere in the same direction to avoid invasive zigzag defect structures, the switching angle is now less than 2θ, which lowers brightness and contrast.

forced to abandon the LCD work in the middle of their FLC success and instead switch to microtip display technology it was, in my opinion, an unmotivated management move. In Japan many companies were involved in the beginning but unfortunately there were no collaborations of the kind that we could later witness in the development of the TFT technology.

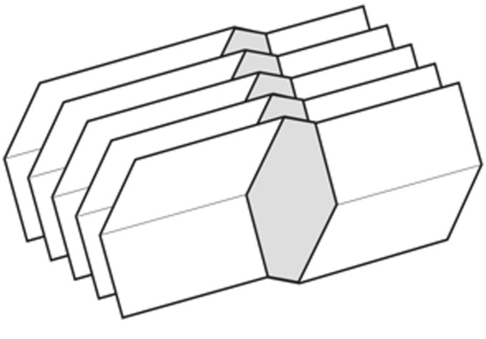

Figure 13. C1 and C2 chevrons have folds in opposite directions and are joined by upright lozenge-like parts propagating like straight lines (that zigzag through the structure). The electrooptic properties are marred by the fact that for a nonzero pretilt the C1 and C2 areas give different contrasts, and the zigzag lines give yet a third contrast. From [40].

The first practical demonstration of a bistable liquid crystal device was based on the SSFLC structure (Canon Inc. Tokyo, 1989). It was also the first demonstration of in-plane switching, demonstrating the superior viewing angle and inspiring later developments (IPS) using nematics. The Canon project was very ambitious. Step by step they mastered all difficulties: the narrow cell gap, symmetric bistability, homogeneous chevron structure, layer fragility, sticking … in the end they had to design their own chemistry – with less good result.

The high-resolution color display that Canon brought on the market in 1995 was outstanding at that time, also considering its size, but it was quite expensive. The manufacturing had a limited volume and three years later when sales had been constantly low on the Japanese market the operations were discontinued due to the competition from TFT displays. These were not only cheaper but, eventually, had also a superior performance. At that time Canon instead increased their stake in microtip technology (called SED), a project that had started at the same time as the FLC project. More than 10 years later the massive SED venture has not led to any commercial products, and since 2007 Canon is now also pursuing OLED technology.

Surprizingly, the FLC failure was not due to low production yield. A key factor was FLC chemistry. The dominating chemical companies had since long concentrated their efforts on tailoring the more accessible nematic materials, and with the promise of TFT technology, the further work on FLC materials was essentially stopped. The SmC* phase of the material used by Canon had a relatively broad range of stability but was in fact metastable at the temperature of –40°C, typically attained in air transport. Although the supercooled smectic phase never crystallized in those few cases where the display was sent to Europe and to USA, the company obviously was not prepared to take this risk.

As a result the display was not marketed outside of Japan. The display is shown in Figure 14. It had 1280 × 1024 pixels, each divided in four subpixels (red, green, blue, white) capable of generating 16 colors. It used a C1 chevron structure with very high surface pretilt (18°) – achieved by a special aligning polymer – and a cell gap of 1.1 μm, which required a *tour de force* in manufacturing technology. The half tones are generated by spatial dither technique. High quality rendition of artwork is extremely sensitive to flicker. The FLC freedom of flicker – at that time a novelty thanks to the bistability – therefore gives an unusual means of presenting art, here illustrated by the Dining Room by Bonnard and by the self-portrait of the Polish turn-of-the-century artist Wyspianski.

SSFLC devices may also be manufactured in polymer form as pioneered by Idemitsu Kosan Ltd, Tokyo. Development of this technology began in 1985, at the same time as Canon's FLC project. The material is a comb-shaped polymer with conventional rodlike SmC* units connected to the polymer main-chain (usually polysiloxane) by flexible spacers. The polymer is laminated between two plastic substrates with insulating layers and transparent ITO electrodes (0.05 μm). Manufacturing takes place in a conveyor-belt process and alignment is accomplished by shearing between rollers after laminating. No alignment layers are thus used. This gives a light-weight, flexible and unbreakable panel. The FLC polymer thickness is 2 μm, defining the cell gap. With polarizers the final display is 0.5 mm thick.

With the recent interest in 3D TV Idemitsu's extremely simple solution with a large area shutter on the front of the TV for production of 3D images may gain a certain actuality. The FLC polymer (FLCP) in this case has to be a strict $\lambda/2$ plate without polarizer, which switches its optic axis by 45° and thereby turns

Figure 14. Canon 15 inch color screen that went into production 1995. The display has 1280 × 1024 pixels, each divided into 4 subpixels. The cell gap is 1.1 μm.

the polarization of every second image from vertical to horizontal. A large sheet polarizer is placed directly on the front of the TV and the observer watches with passive polaroid glasses admitting orthogonal vibrations. Alternating images correspond to right and left eye, thus the stereoscopic TV is driven at double speed (120 Hz instead of 60 Hz). It allows 8 ms for each picture, but in order to avoid any inhomogenities in the image, the response time of the FLCP has to be 1 ms. This is achieved by applying ±15 volts at room temperature. The light transmission is 30% and the contrast better than 100:1, a performance that dates from 1998.

As explained, the Canon display was passively addressed (no transistors). The passive matrix could simply be scanned line by line (at 300–400 lines it would have been capable of video rate) thanks to the bistability and the inherent speed of the SSFLC itself). Another Japanese company that mastered bistability – with a different alignment technique – was Citizen, and this company is still manufacturing simple FLC displays which, due to their bistability, draw ultra-low power. Some examples of Citizen displays are shown in Figure 15. They have of course a much

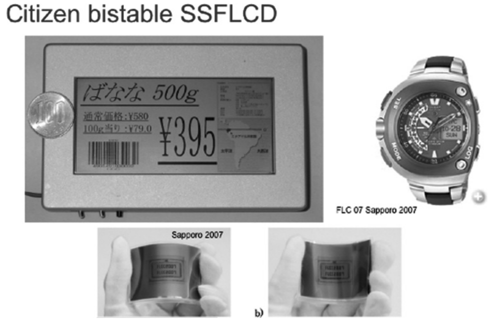

Figure 15. Some examples of hard and flexible bistable passive matrix FLC displays manufactured by Citizen. The monochrome reflective display on top left has a resolution of 1000 dpi (dots per inch). The bistability is achieved by SiO evaporation that gives a high pretilt (about 20°).

better viewing angle than simple TN displays (and no "shadow" on the inner reflecting back side). Citizen, who uses FLC materials engineered by Clariant, also manufactured the sophisticated passively addressed display – a spatial light modulator (SLM) – that is the key processing element in the Agfa MSA Dimax color printing system brought on the market in 1998.

Otherwise, the dominating FLC products on the market today are microdisplays actively addressed from a silicon backplane, which are used as electronic viewers in high-end video and digital cameras and recently in small projectors.

3.5. *Active Matrix FLC*

The first such devices were a joint development between Displaytech, Inc., Colorado, USA and Miyota, Japan. They are now manufactured at about five million displays a year. This production would not have existed today, were it not for a devoted work of small groups to develop FLC chemistry, at Hoechst (later Clariant) in Frankfurt, at 3M in St. Paul, Minnesota, but in particular at Displaytech (now a branch of the semiconductor company Micron) where it was clear that the company would not survive if it were dependent on materials from outside and therefore established its own chemistry group from the start. With the support of academic groups in USA and Canada (D. Walba and R. Lemieux) materials with much higher performance have been developed, not only in terms of temperature range and higher speed but also in a long way towards avoiding chevrons.

In the FLC-on-silicon microdisplays the FLC operates in reflection addressed by VLSI CMOS technology. Such single chip microdisplays are capable of video speed in full color. The high response speed allows the gray scale to be generated in the time domain. Examples of such microdisplays are shown in Figures 16 and 17. Initially the CMOS had to provide 3 volts but with recent FLC materials about 1 V is sufficient. With RGB LED illumination the Displaytech 800 × 600 chip gives 24 bit color at 60 Hz frame rate (360 Hz RGB field rate). Microdisplays with higher resolution, aimed for HDTV, have been demonstrated in Japan but also by Displaytech and other similar companies like CRL (originally an off-spring of Thorn EMI). The fastest one is a 0.9″ diagonal UXGA (1920 × 1200 pixels) from Sony with the amazing refresh rate of 2.16 kHz.

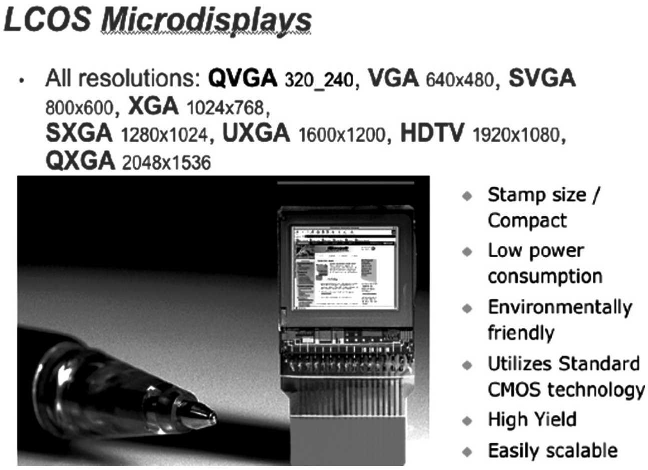

LCOS Microdisplays

- All resolutions: **QVGA** 320_240, **VGA** 640x480, **SVGA** 800x600, **XGA** 1024x768, **SXGA** 1280x1024, **UXGA** 1600x1200, **HDTV** 1920x1080, **QXGA** 2048x1536

- Stamp size / Compact
- Low power consumption
- Environmentally friendly
- Utilizes Standard CMOS technology
- High Yield
- Easily scalable

Figure 16. FLC-on-silicon microdisplay (CRL, Great Britain).

With active addressing it is not necessary to achieve bistability. If the FLC is not driven to latching, analog gray levels may even be produced dynamically by amplitude modulation. This has been used in some versions of FLC spatial light modulators. It is also possible to use entirely different SmC* modes for high resolution video displays in combination with silicon backplanes or TFTs. In fact, at the end of their FLC project Canon, in collaboration with Clariant, demonstrated a 14 inch TFT panel in VGA (640 × 480) resolution working with a monostable surface-stabilized structure of an N*-C* material in a so-called Half-V mode [26]. Also here the chemistry was far from sufficiently developed for a realistic device at the time when the project was abandoned: the range of stability of the C* phase was only from −7°C to +61°C. Dai Nippon Printing showed a 3 inch VGA display using this mode with field-sequential color at the FLC 2007 conference in Sapporo, Japan. The interesting thing with their demonstration was the new filling technique. Large LCDs are today filled by a kind of "sprinkling" method called one-drop filling (ODF). This method could also be adopted for FLC: at 90°C in the N* phase, close to the clearing point, small droplets were dotted by inkjet printing onto the heated (90°C) substrate in 20 μm intervals. It works without creating defects and is probably a realistic way of filling future large FLC displays.

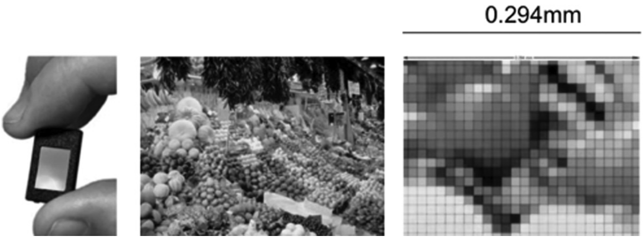

Figure 17. Three views of an 800 × 600 microdisplay made by Displaytech, Inc. At the close-up to the right one can see that the whole area of every pixel is contributing to the image with its true color and brightness, a result of the field-sequential color technique.

In the Figures 17–20 some examples are given of commercial products using FLC microdisplays. Electronic viewfinders for video cameras and later high-end digital cameras have been manufactured since quite a while (Figure 18). More recent is the application in pocket projectors. In Figure 19 is shown such a projector from 3M. It is battery driven, capable of projecting pictures of moderate size and the projection chip can in principle be integrated in a mobile phone.

A particularly interesting high-tech application is the holographic projector made by the company Light Blue Optics (LBO) in Cambridge, England (Figure 20). It uses three FLC displays each of which is a reconfigurable binary phase hologram illuminated by coherent light. Three semiconductor lasers generate diffraction patterns that merge and in real time build up the frames in the full color video film displayed on a screen. There is no gray scale – it is in the diffraction pattern. In this device there is no need for blanking as in other FLC devices, because the diffraction pattern for data and inverted data is the same, so you can just invert the signal after every frame and keep fully DC-compensated driving. Furthermore the projector does not need any focusing – the picture is sharp in every plane that you put in the light cone (Fraunhofer diffraction). An image in the video film is built up of many diffraction patterns acting as kind of subframes. In order to update the diffraction patterns electronically the liquid crystal in the display has to react very fast – only FLC could do that.

An interesting technique that has now become very wide-spread in the last decade is the polymer-stabilization of different liquid crystalline materials, the last example being the remarkable polymer-stabilization of the blue phase worked out by H. Kikuchi. In the SmC* case the liquid crystal is first surface-stabilized, then polymer-stabilized in the surface-stabilized state, which can be done in a variety of ways. For instance, the UV radiation can be applied while the FLC has been switched to one of its to stable states and is being held in this state. The resulting polymer-stabilized FLC will then become monostable and is capable of electro-optic

Figure 18. Minolta Dimage 7 and Hewlett-Packard Photosmart – two examples of digital cameras equipped by FLC electronic viewfinders displaying the actual image on the CCD. Hence you can pre-check the actual image even in bright sunlight (as you used to be able to in old cameras).

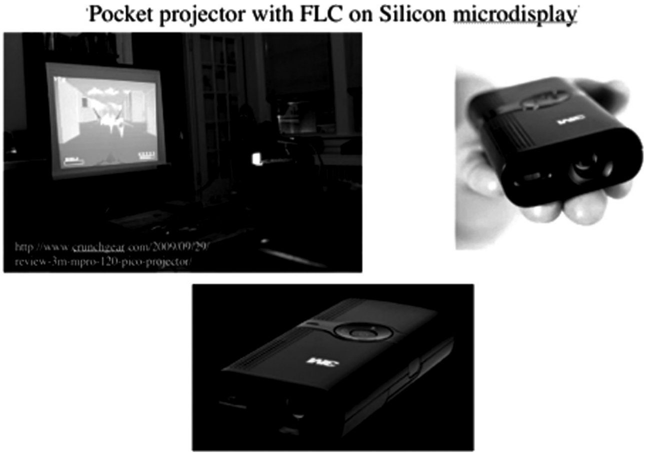

Figure 19. Battery-driven pocket projector from 3 M that came on the market 2009.

response with a certain grayscale. If, on the other hand, the UV illumination is taking place stroboscopically in phase while the FLC is being switched back and forth between the end states, a symmetric but steep hysteresis curve may be achieved. Different kinds of electro-optic response and hysteresis loop will result depending on the structure of the initial surface-stabilized state and the mode of illumination. An interesting example is the polymer-stabilized V-shape mode worked out by S. Kobayashi and coworkers together with Dainippon Ink & Chemicals (DNC) [38]. A small (4 inch) SVGA (800 × 600) field sequential color video rate direct view display has been demonstrated. It is monostable and has a symmetric analog but non-linear switching around zero voltage, not to be mixed up with the linear mode in helical smectic C^*.

Assessment. Of all electro-optic effects described in this review are those based on FLC, so far, the only ones that have led to commercial products. If they will lead

Figure 20. Light Blue Optics' holographic projector and its image on a table. There are no polarizers and hardly any optics. There is no focusing and no need for blanking.

to macrodisplays and not only to microdisplays is a different question but they would certainly be the leading candidates. While they would not compete at the giant LCD sizes, there is a whole range from dvd-players to domestic TVs up to perhaps 30–40 inch where their high spatial resolution would be an asset. What speaks for FLC is that material engineering at least has advanced sufficiently far that one can really work with low voltages and, at such low voltages, FLC is superior to other liquid crystal technologies in speed. Hence they are well suited for field-sequential color. However, there is a lot more to do in materials development. Displaytech's well-engineered materials are adjusted to reflective mode so new materials should also be developed for at least twice the present cell gap. Many initial problems have by now been solved, but some remain. Chevron structure still causes the tilt angle to be about 15° rather than the optimum tilt angle 22.5°, which reduces the efficiency of the backlight. On the other hand, a 15°C* switches twice as fast as when $\theta = 22.5°$. Likewise a high-P material switches faster but draws higher power. A number of such considerations have to be taken into account. Thus we opt for low-P materials but with non-chevron structures and with lower viscosities to compensate for the larger switching angles. This kind of optimization of the important parameters has essentially been done already in nematics. Polymer stabilization is by now a routine in manufacturing industry and makes the smectic structure less fragile. The recent progress in de Vries-type materials is very encouraging but as these lack a nematic phase they have to be aligned directly via the isotropic-smectic A* transition. This is a new alignment problem that has to be studied.

3.6. *Antiferroelectric Liquid Crystals*

In addition to the SmC* phase, in which the tilt is synclinic, i.e., essentially in the same direction (the presence of the helix means a shift in direction of typically half a degree from layer to layer) there is also an important polar smectic phase where the order is anticlinic, i.e., with tilt alternating between opposite directions from layer to layer. This was independently recognized by Japanese and French researchers and reported at the 1989 FLC conference in Göteborg [27]. The phase is designated SmC_a^* (the index stands for anticlinic) and its structure is shown to the right in Figure 21, ignoring for the moment its helical superstructure. Because of the alternating tilt, the local polarization also alternates from into to out of the paper plane as shown. In principle there should also exist a corresponding non-chiral $\mathrm{C_a}$ phase that is non-polar, built-up of non-chiral molecules, but substances showing this phase seem to be extremely rare. They have been reported in only a couple of very special (swallow-tail) molecules. This may point to the fact that the spontaneous polarization plays an important role in the appearance of anticlinic order, corroborated by the fact that P normally has a much higher value in C_a^* compounds than in compounds only showing the C* phase. When they both appear, the C_a^* phase is found below C* and the tilt is higher, often about 30° instead of around 20° more typical for the C* phase. The C_a^* phase is also almost always much more hard-twisted than the C* phase with a helical pitch not seldom of the order of 0.1 μm.

In the C_a^* phase the polarization is already cancelled on a molecular level as the $\boldsymbol{P}$ vectors in adjacent smectic layers are antiparallel to each other. The macroscopic polarization of the anticlinic structure is thus zero and we therefore call the smectic C_a^* an antiferroelectric liquid crystal (AFLC). It has, in its surface-stabilized form,

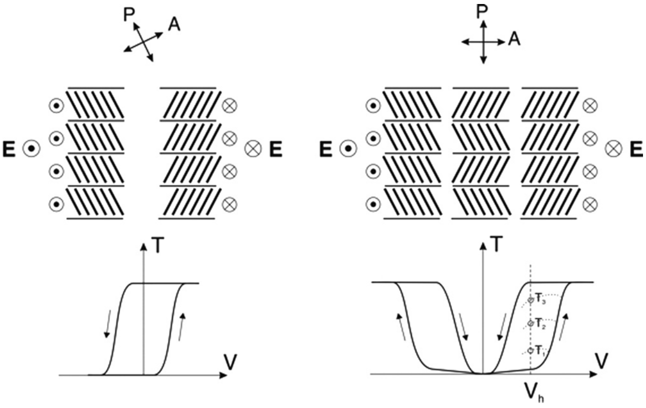

Figure 21. Electro-optic effects in surface-stabilized FLC and AFLC structures. The FLC case to the left is repeated from Figure 9 in order to emphasize the difference in polarizer setting. Right: the electro-optic switching of a surface-stabilized antiferroelectric liquid crystal is characterized by a double hysteresis loop. Because the transmission T is symmetric around $E=0$, an AFLC display can in principle be driven without DC bias in almost the same simple manner as a nematic display, by reversing the sign of E between successive frames. It further allows (in principle) a simple rendition of gray states. The polarizer setting is such that the dark state is the $E=0$ state with an optic axis along the layer normal, independent of temperature, whereas the dark state in the FLC case is one of the synclinic states which are necessarily dependent on temperature as the tilt θ depends on temperature. From [40].

the typical electro-optic response of a solid antiferroelectric with a double-loop hysteresis as illustrated in the figure. Like the SmC* phase, the SmC_a^* is also helical in the bulk (i.e., it has a helical superstructure) and in this state both phases are positive uniaxial with the optic axis along the layer normal. In its surface-stabilized state, which is the preferred structure for devices, the anticlinic structure is biaxial, with the two optic axes lying fairly close to and on either side of the layer normal in a plane perpendicular to the tilt plane. Seen from above, i.e., looking through a display as in Figure 21, the effective optic axis is the slow axis of the indicatrix, which is along the layer normal. Therefore, with polarizer and analyzer set as in the figure, we have a black state for $V=0$. It is switched into two equivalent bright states for $\pm V$ being higher than a certain threshold. This way of writing a state not only eliminates the DC bias which is a problem in FLC addressing but offers a simple way to generate a gray scale by amplitude modulation as discussed below. For high values of V the material is entirely switched to the synclinic state, symbolically AF→F. This is *not* a field-induced phase transition from SmC_a^* to SmC* as is a common misstatement. The material is still in its antiferroelectric *phase* but in its ferroelectric *state*. The fact that an antiferroelectric can be switched into its so-called ferroelectric state is a basic element in the definition of an antiferroelectric.

In contrast to the bistable SSFLC, the SSAFLC is monostable and relaxes back to the only stable state – the anticlinic state – when the field is taken off. This can be taken advantage of if we apply a holding voltage $\pm V_h$ after the switching pulse. As illustrated in the figure, three different amplitudes in this switching pulse give rise to three different transmission levels (T_1, T_2, T_3) when the back relaxation is stopped by the holding voltage. The different levels correspond to three different fractions of area coverage made up by synclinic (bright) microdomains embedded in anticlinic (dark) microdomains. In this way, an analog gray scale can, in principle, be written. Reliable gray levels require a very high degree of symmetry and stability of the hysteresis loop, and with many gray levels the degree of sophistication increases, also in the addressing waveforms. Furthermore, the special form of "quasi-AC" driving requires high switching rates in order to eliminate flicker.

Surface stabilization is a special problem in the case of AFLC. We already mentioned that the helical pitch p normally is much smaller than in the AFLC case. One can make the pitch long enough in well-engineered mixtures (for instance the Chisso AFLC material CS 4001 has a pitch of 2.8 μm at room temperature) but, in particular, single compounds may be very hard to surface-stabilize. This is aggravated by two circumstances. First the surfaces are not so efficient for unwinding the helix in AFLC as they are in FLC because no surface really promotes the anticlinic structure while it may well promote the synclinic structure. Second, the symmetry of an AFLC shares the property of a cholesteric that the physical period is actually half the pitch. Therefore, the critical cell thickness should rather be comparable to $p/2$ than to the full pitch p. This means, in essence, that *it is harder to surface-stabilize an AFLC than an FLC*. In order to take the pains to go to extremely thin cells, which requires considerable experimental skills, you really have to know why you are doing it. In most academic research on AFLC so far the authors do not seem to be aware of the problem with surface-stabilization.The idea or conception is rarely even mentioned – as rarely as pitch values are stated.

With a well-defined dark state independent on temperature, with easy DC compensation and analog gray scale, the AFLC technology seems to combine some of the best features from both smectics and nematics. It was also believed that AFLC had less sticking problems than FLC due to the AC-like driving and the non-polarity of the dark state (probably true), a self-healing ability against mechanical layer damage (quite possible) and no chevron problems (definitely untrue). Some drawbacks compared to FLC were also admitted: the alignment was not very good with a high density of characteristic microscopic defects. This was reported to be due to the phase sequence Isotropic – A^*-C^*-C^*_a, in other words, there was no nematic phase. For some strange reason this phase – which was thought to be a key factor for good alignment – never appeared in any AFLC substance. The statement that there are no chevrons in the AFLC was a mistake based on the fact that no zig-zag defects could be observed. But there were some other problems: due to the higher polarization the power consumption is rather high (especially since there is no bistability), the switching is a little slower than in FLC but, in particular, the back relaxation to the black state is much slower since no field is acting. (This reminds about the nematic case.) The back switching can, however, be made faster by devoted waveforms (kick-back pulse). As these problems could be overcome, after all, the AFLC technology looked promising enough to take over at least a great share of the market that was foreseen for the FLC project, which had started five years earlier. Very ambitious synthetical chemistry programs were begun in Japan (Showa Shell Sekiyu and Mitsubishi Gas Chemical), which in a very short time led to excellent materials. Based on these, good color display prototypes of increasing size were developed by Denso Corporation from 1991 to 1997. Citizen, always interested in passively addressed displays had also presented smaller but quite attractive black and white prototypes.

Two of the Denso displays are shown in Figure 22. These passively driven displays could perhaps not compete with the more sophisticated Canon displays but

Figure 22. Two examples of AFLC display prototypes from Denso Corporation; (top) two views of a 6" screen scanning 220 lines at a refresh rate of 60 Hz demonstrated in 1993. The stated contrast ratio is 23:1; (below) video display of same size and resolution demonstrated in 1995 with a somewhat higher refresh rate and contrast 30:1. In 1998 Denso also demonstrated good 17" desktop models with 1200 lines for static pictures (though less sophisticated than the Canon displays).

were very bright and had quite good color rendition. The small ones (6") had video speed (at 220 scanning lines).

While the FLC synthetic activity peaked around 1990–1992, the AFLC synthetic activity peaked about 1996–1998. In 1998 Mitsubishi announced that they were going to start big volume production of well-engineered AFLC mixtures in 1999. Then nothing happened. After a year the whole AFLC activity in Japan had stopped. The displays never reached manufacturing. At that time the investments already in chemistry alone had amounted to more than 100 million US dollars. What happened? Nobody knows for sure because the big companies normally do not analyze their failures in public. Hence, what follows is a subjective attempt to analyze the facts.

3.7. *Why Are There Still No AFLC Displays?*

There are some more differences between the SmC* phase and the SmC_a^* phase that we have not discussed so far. For instance, in the AFLC case there is no useful mode corresponding to DHM (section 2.3). In fact, helix unwinding is a completely different process in SmC_a^* than in SmC* and the whole process from the helical groundstate to the fully switched state is quite complicated. Even ignoring the helix we will find that the process is of a different nature and that it is, at least, a two-step process. Assume, for instance, that a field is applied across the cell in the anticlinic state of Figure 21 and that the tilt plane is strictly parallel to the glass plates. At first nothing will happen since E is collinear with P and does not exert any torque on the molecules. This situation is, however, unstable and when we raise the field to a certain level (actually a voltage threshold) a kind of Frederiks transition will occur at which the tilt plane will bulge out and start to turn. The local order is essentially still anticlinic. The local switching from anticlinic to synclinic state is a different process taking place at higher fields (with a field threshold). These field-induced transitions have been investigated both theoretically and experimentally, especially by the group at Case Western in Cleveland and the group in Oxford [28]. If the helix is present at the start its unwinding will further complicate the process and the hysteresis curve may have a linear part at low fields that may be quite pronounced. But before the anticlinic → synclinic switching takes place we end up in an intermediate state with an (essentially) non-helical anticlinic structure with the tilt plane *perpendicular* to the glass pates. What we cannot achieve, in contrast, by applying an electric field, is the anticlinic structure with the tilt plane parallel to the glass plates as in Figure 21. This has important consequences. It means that while to the left (FLC case) we could realize the states with the directors in a plane parallel to the cell plates by electric field unwinding as well as elastic unwinding, this is not so to the right (AFLC case). The non-helical anticlinic state parallel to the cell plates can *only* be achieved by *elastic unwinding*. It means that one has to be particularly careful with surface-stabilization in an AFLC. In the FLC case hysteretic effects caused by dynamic driving will help up a surface-stabilization that is not perfect while in the AFLC case the driving pulses will not be helpful at all.

The linear part of the hysteresis loop that sets in immediately at low fields (the pre-transitional regime) causes a dynamic light leakage in every switching process. But it turns out that there is an even more serious *static* light leakage. This is due to chevrons, which in the AFLC case appear in a different way than in FLC devices. The reason for the chevrons in both cases is that the layer structure first forms in the SmA* phase, and that the initially straight layers fold in the middle of the sample when the layer thickness shrinks as a result of the molecular tilt in the SmC* or SmC$_a^*$ phase. As is evident from Figure 11, the $\boldsymbol{P}$ vector is not any longer along the applied electric field in the case of chevrons, and due to the high P value in AFLCs, the torque from $\boldsymbol{E}$ is strong enough to straighten up the layers to be vertical. However, in order to fill out space, the layers then have to buckle along the horizontal direction. This is shown to the left in Figure 23. Thus we do not have any uniform layer normal (optic axis) any longer, and no setting of polarizers can give a sufficiently good dark state. In essence we get a bookshelf configuration with two main layer directions with optic axes equally offset the optimum polarizer setting. Light is always leaking through in the zero-field (OFF) state, and the problem is even aggravated under driving conditions. This seriously limits the achievable contrast in an AFLC display. If we look at the published specifications for the Denso displays we find a contrast ratio of 20:1, 23:1 and 30:1, surprisingly low values. That the displays nevertheless looked quite good is due to the excellent transmission in the bright states. But the contrast is far from sufficient due to the inadequate dark state. If we add the two contributions to the light leakage as shown in the upper right part of Figure 23 we find an upper bound for the achievable contrast to be about 50:1 for typical AFLC displays. If the pre-transitionally effect could be eliminated, one might come closer to 100:1, but any lack of symmetry in the switching would also reduce the contrast.

3.8. *The Orthoconic AFLC*

At the end of the 1990s it was realized [29] that the serious main problem with the AFLC dark state can be solved by using a material with $\theta = 45°$. When θ approaches

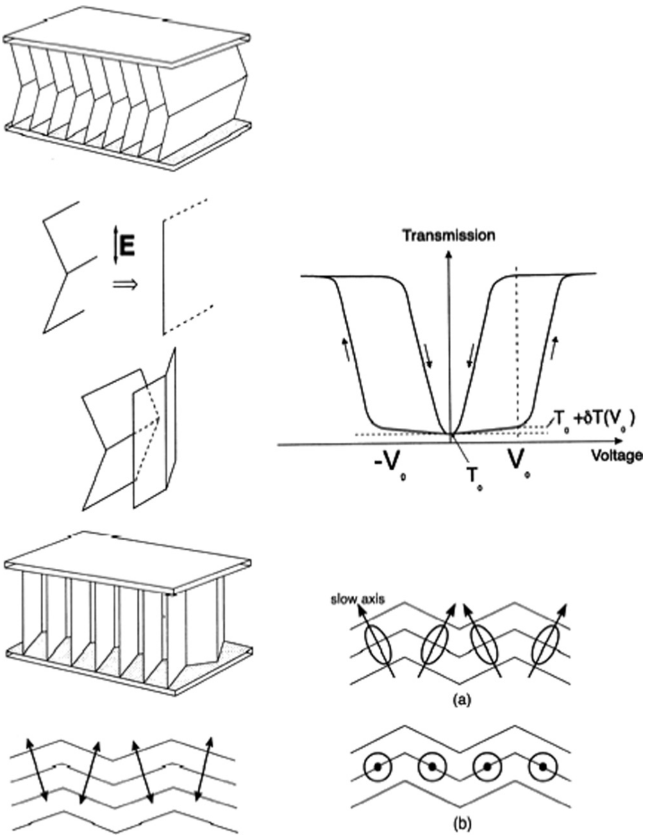

Figure 23. Shrinking of the smectic layers on decreasing the temperature leads to horizontal folds (vertical chevrons). An electric field applied across the electrodes straightens up the chevrons, forcing the folds to become vertical (horizontal chevrons). The result is kinks in layer direction (left). The transmission through the cell becomes non-zero even for $V = 0$ (upper right).

45° the optical properties of the surface-stabilized AFLC structure in Figure 21 changes dramatically: instead of being biaxial positive with the slow axis along the layer normal it becomes uniaxial negative with the optic axis perpendicular to the layer normal. (Such a transformation could only happen in a liquid crystal.) The SSAFLC now behaves as a perfectly homeotropic nematic, independently of how the smectic layers buckle and curve in the plane of the paper, and hence gives a perfect black state. This is illustrated at bottom right of Figure 23: (a) shows the situation corresponding to $\theta = 30°$, in (b) $\theta = 45°$ and the optic axis points out of the paper instead of being along the layer normal. The extinction in this state is extremely good and the dark state has the same viewing angle as in a VAN display – without any sophisticated surface treatment whatsoever. We call such a surface-stabilized 45° AFLC *orthoconic* (for short OAFLC or simpler OAF), as the cone apex angle is 90° and the optic axis is orthogonal to the cone axis (layer normal). The switching properties of the orthoconic smectic are also unique. Conceived as a $\lambda/2$ plate and with polarizer setting as in Figure 21, it switches between the black state and the two brightest states that can be achieved between polarizers.

The contrast and brightness of OAF devices is therefore outstanding. The most powerful mode is to use the orthoconic between crossed *circular* polarizers (such as used for watching 3D movies like *Avatar*), as in this case even the transmission in the bright state is independent of any misalignment in the smectic layers. The OAF is also ideally suited for reflective devices of high contrast and brightness.

During the industrial development of AFLC displays it was often said that the bad darkstate was "a difficult alignment problem" because the materials lacked a nematic phase, and great efforts were made to develop AFLC materials having the nematic phase, in vain. And it is true: AFLCs do not have a nematic phase. The reason is the same as in the case of de Vries-type smectics [14]. But even if they had had an N phase this would not have helped against the layer buckling instability. Orthoconics thus do not solve an alignment problem, they circumvent it.

In order to be useful at all a material cannot, of course, have $\theta = 45°$ at just one temperature but must satisfy the orthoconic condition over a large range of temperature, including room temperature. R. Dabrowski and his graduate student W. Drzewinski at the Military University in Warsaw were able to design such a mixture, W 107, with $\theta \approx 45°$ over a temperature interval of more than 60 degrees on which the unique optical properties described above could be verified. (W in this case stands for Warsaw.) It has a phase sequence Isotropic – SmA*-SmC*-SmC$_a^*$ – Crystal with a strongly first order transition SmA*-SmC*. It would be practically excluded to make a 45° AFLC with a second order tilting transition, because in such a case the tilt typically saturates around 25° in the C* phase and then does not increase very much further in the underlying C$_a^*$ phase. An important question is now how big deviations from $\theta = 45°$ we could tolerate and still have an essentially perfect darkstate. This is answered in Figure 24 that shows results of contrast calculations by P Rudquist for two values of layer misfit as illustrated at the bottom of Figure 23. Assuming perfect polarizers we see that for deviations in θ of $\pm 2°$ a very high contrast is achieved even for layer misfits as large as $\pm 10°$. The closer we come to 45° the larger the misfit that can be tolerated and for θ exactly 45° the contrast is infinite whatever the misfit.

W 107 was not the first AFLC material with a tilt of 45° or thereabout. The first material, later called MHTAC, with a tilt θ close to 45° was reported in an X-ray study by A.M. Levelut *et al.* [31] in 1983 but no electro-optic study was undertaken. The first report of an AFLC with $\theta = 45°$, even over a large temperature interval, was published in a British patent by H.J. Coles *et al.* from 1996, and Coles' group, which contained both physicists and chemists, worked intensely with such materials during the latter half of the 1990s [32]. However, it turned out that the only advantage of these special materials was their large switching angle, otherwise they behaved exactly like the Denso materials, only being slower and showing a huge pretransitional effect that seriously reduces the contrast. (In [32] contrast values like 100:1 are claimed, although it seems reasonable if they were lower than the values reported by Denso, cf Figure 22.) But in principle, at least some of Coles' materials are orthoconic. Only, their orthoconic properties were never discovered, since the materials were never surface-stabilized. Therefore, as can be verified in the different papers of [32], the optic axis is always along the layer normal. The huge pre-transitional effect is probably due to the fact that the helix unwinds as the first part of the switching.

When writing up a feature article on orthoconic materials [33] the Chalmers group made a search in more detail of the earlier literature. We then found that

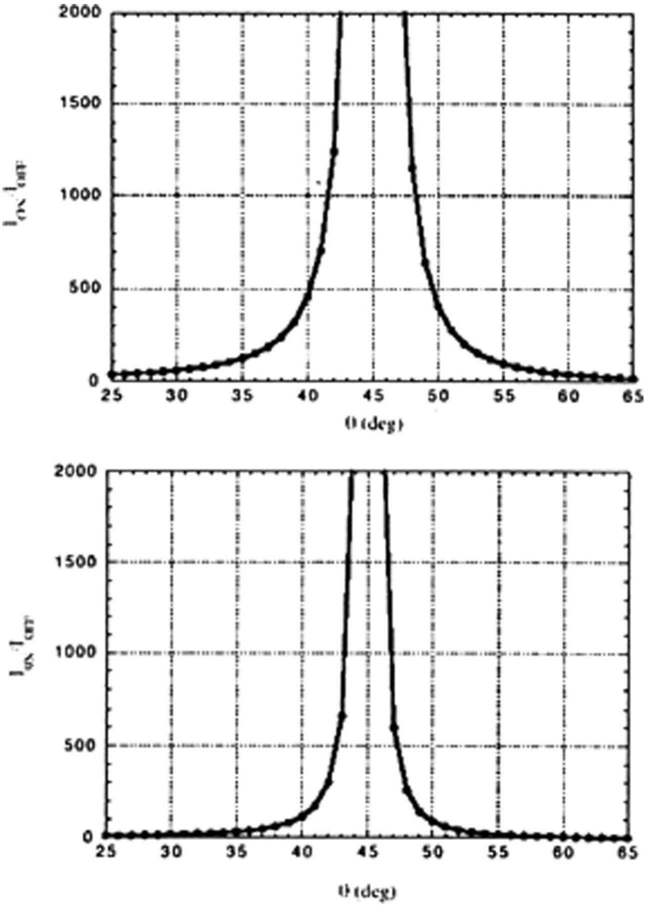

Figure 24. Contrast between the ON and OFF states as a function of tilt θ for the SSAFLC structure in Figure 21 (horizontal tilt plane) between ideal crossed polarizers, for two values of layer misalignment: 5° (top) and 10° (bottom). From reference [30].

the peculiar feature that an anticlinic structure with 45° tilt should have a vanishing birefringence in the tilt plane had been stated already in 1970, in one of the first papers dealing with the optical properties of smectics [34]. This was even long before antiferroelectric liquid crystals had been found. It was again, and very clearly, stated in 1996 although in a theoretical paper dealing with diffraction gratings [35]. It is not too surprising that these papers both remained unnoticed by everybody working with the subject of AFLC. In fact, we were the first to observe these papers in this context and the first to quote them [33].

While the Dabrowski mixture W 107 has been instrumental for the first demonstration of the optical properties in the orthoconic condition, it is not the perfect material. First of all the helical pitch is too tight, $<0.4\,\mu m$ at room temperature. This requires sub-μm thin cells to obtain good surface-stabilization. In order for an orthoconic material to be practical this value of pitch must be increased by a factor of five or ten. In spite of several European projects among academic groups, where this has been an issue, no such materials have been produced so far. The experience is that the tilt decreases when the pitch gets longer. It is hard to judge if this is really an intrinsically difficult problem or not. Anyway those projects were helpful in showing that high-tilt AFLCs must not necessarily be connected with a high value of polarization. Adjusting other material parameters to fit cell gaps of 2–3 μm should be a minor problem.

Assessment. As already stated AFLC technology should have had several important advantages over FLC technology. It is then important to analyze the factors behind the failure. In addition to the dark state there have been other kinds of problem. The hardest was probably the analog gray scale that looks simple in theory but requires a delicate reset to the same stable dark state in each switching process. With a conventional AFLC there are, in fact, only two states that could be considered stable, the two symmetric synclinic end states, which both represent white. With orthoconic antiferroelectric materials also the black state is well defined. Thus OAF has the great advantage over FLC of a much superior black state that is, moreover, *temperature independent* – requires no special setting of the polarizers. The most promising way to use the OAF potential is now therefore to abandon the analog gray scale and generate the gray levels in time instead of using microdomain switching. This means to use only the black and white states as in FLC. This eliminates the difficulties in achieving perfect symmetry and also the complicated temperature dependence of all involved processes. Together with the outstanding quality of the black and white states it keeps the simple DC compensation and allows simple addressing wave forms. With active matrix driving the OAF is sufficiently fast that the gray levels can be generated in time. Furthermore the voltage required for switching becomes much lower as the threshold is dynamic just as in the FLC case.

3.9. *Other Tilted Smectics*

There exist other tilted smectics than the synclinic SmC* and the anticlinic Sm C$_a^*$. Descending from the A* phase the following phases have been reported: A*-C$_\alpha^*$-C*-FI$_2$-FI$_1$-C$_a^*$, and sometimes many more, most of which can safely be considered experimental artifacts resulting from sloppy and badly understood switching measurements (“one peak” or “two peaks” in the current response). Such measurements can never yield details about the mesoscopic structure – as a minimum they have to be combined with dielectric spectroscopy. The only quite reliable method is resonant X-ray scattering. There seems to be five tilted smectics (or perhaps one more but that question is still rather academic) and the three less common ones are sometimes called *subphases*, sometimes *intermediate* phases since they are supposed to be in some way intermediate between the synclinic C* and the anticlinic C$_a^*$. The question is now: how interesting are these phases for future applications, particularly for displays? The first of the phases, the C$_\alpha^*$ has the same structure, helielectric, as C* but with extremely short pitch (not more than 5–8 layers) which is possible as the tilt angle is also extremely small. It has among other things been given the nonsensical name “mixed antiferroelectric-ferrielectric” although such properties could not possibly even be verified. The phase FI$_2$ is, according to the name, ferr*i*electric, but we know that in reality it is antiferroelectric – if anything (since it would be hard to verify experimentally). But the name FI$_2$ seems to stick which shows that liquid crystal researchers do not have the same nor even consistent vocabulary. The FI$_1$ has a mesoscopic polarization and might exhibit ferrielectric properties under surface-stabilized conditions. This is also the phase that has been highlighted for applications, as it in principle then could be switched between more than two states. But the problem is that all intermediate structures are in conflict with the surfaces, even more so than C_a^*. In fact they are unstable and vanish completely in thin cells. Quite apart from their scarce availability and narrow temperature stability this makes them academic curiosities rather than materials for device applications.

3.10. *The Problem of Hysteresis*

The electro-optic effect of FLCs is based on the hysteretic loop as illustrated in Figure 21. It is a single loop and only the outer $\pm V$ states are written. As reversal of the sign of V everywhere does not give the same picture every frame has to be electrically compensated by some kind of blanking frame. Otherwise this kind of hysteresis is no disadvantage except that, since the tilt depends on temperature, the crossed polarizers have to be set for the black state corresponding to the typical operation temperature. It is an important part in the definition of ferroelectricity that the polarization is observed as a two-valued function of the applied electric field [39]. This feature then here shows up as a two-valued optical transmission as a function of applied voltage. This is in fact the meaning of hysteresis and is here a *good* thing. The device is based on it.

In the AFLC case we have a double loop and blanking is inherent by using a frame and its reverse for writing a single picture. Here it seems that the black state is independent of temperature. But the reality is more complicated. First of all since not only the outer parts of the loop are used but all sub-loops in between corresponding to different levels of gray. To see the problem more clearly, look at Figure 25 where a transmission-voltage curve has been traced that could, in principle, represent almost any kind of electro-optic effect. For the corresponding device to work well this curve *should not* exhibit hysteresis.

But it often does. For nematics which are 3D liquids this hysteresis can mostly be ignored. In other cases it can be a serious problem. We already saw in chapter 2.3 how hysteretic effects destroyed the viability of the deformed-helix mode. It can also be a problem in a monostable polymer-stabilized FLC where the grey shade ought to be a mono-valued function of V. Thus the half-V-shaped and the V-shaped switching modes have to face this problem. It appears likewise in the writing of gray shades in AFLC where furthermore deviations from perfect symmetry around the T axis (like in V-shape switching) is an additional problem. Hysteresis is certainly an inherent

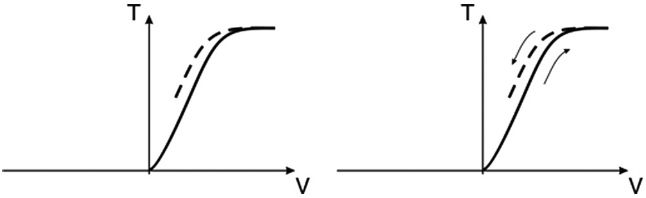

Figure 25. Transmission-voltage curves for an electro-optic effect that ideally should not show hysteretic effects but in reality does. The illustration to the left shows how the T-V curve may change behavior upon age, for instance after many cycles of switching, while the illustration at right shows that the same curve is not traced when V is increased as when decreased.

feature of microdomain switching. Generally speaking, any switching that strains some kind of lattice or rigid structure, like a polymer-stabilized structure, is susceptible to both directional hysteresis as well as fatigue hysteresis. Thus these problems appear also in the blue phase displays, in fact in anything that is not nematic, and creates a problem for the gray scale. With strong hysteretic effect even the dark state tends not to be well defined any more. This favors fast digital techniques like FLC, and OAF ought to be employed similarly as already stated.

4. Summing Up

Can liquid crystals other than nematics be useful for devices, notably displays? As passive matrix addressing already belongs to history except for simple displays, the opportunity may have come when the manufacturing industry of high resolution displays now goes from color filters to field-sequential color. Speed is here the key factor. FSC is just barely possible with nematics in reflective microdisplays with very narrow cell gap but hard to obtain in large transmissive displays. FSC fits very well with digital techniques. Ferroelectric liquid crystals, combining high speed with very low switching voltages and with a fair maturity in materials engineering development, is one of the candidates at the side of the blue phase. An interesting runner-up is the orthoconic antiferroelectric liquid crystal (OAF) combining reasonably high speed with superior contrast and viewing angle in spite of the simplest surface treatment. This has led to a new interest in AFLC although the development of engineered materials showing the orthoconic condition has only just begun. For non-display applications (at least) a closer look ought to be taken into the electroclinic effect after the recent progress in de Vries-like materials. To sum up: you cannot do anything without adequate and supporting chemistry but physics may help to find out the direction.

Acknowledgment

The author wishes to thank Professor Per Rudquist, now head of the Chalmers Liquid Crystal Group, for many fruitful discussions.

References

[1] Brody, T. P. (1996). The birth and early childhood of active matrix. *Journal of the SID*, *4/3*, 113.

[2] Schiekel, M. F., & Fahrenschon, K. (1971). Deformation of nematic liquid crystals with vertical orientation in electrical fields. *Appl. Phys. Lett.*, *19*, 391. (DAP: Deformation of Aligned Phases)

[3] Patel, J. S., & Meyer, R. B. (1987). *Phys. Rev. Lett.*, *58*, 1538.

[4] Patel, J. S., & Lee, Sin-Doo (1989). *J. Appl. Phys.*, *66*, 1879.

[5] Lee, Sin-Doo, & Patel, J. S. (1990). *J. Appl. Phys.*, *67*, 1293.

[6] Rudquist, P., Komitov, L., & Lagerwall, S. T. (1994). *Phys. Rev. E*, *50*, 4735.

[7] Rudquist, P., Carlsson, T., Komitov, L., & Lagerwall, S. T. (1997). *Liq. Cryst.*, *22*, 445.

[8] Rudquist, P. (1997). *The Flexoelectro-Optic Effect in Cholesteric Liquid Crystals*, PhD Thesis, Chalmers University of Technology, Göteborg.

[9] Lagerwall, S. T. (1999). *Ferroelectric and Antiferroelectric Liquid Crystals*, Wiley-VCH: Weinheim.

[10] Garoff, S., & Meyer, R. B. (1977). *Phys. Rev. Lett.*, *38*, 848.

[11] Ratna, B. R., *et al.* (1998). *Proc. SPIE*, *3297*, 2.

[12] Kapernaum, N., Walba, D., Korblova, E., Zhu, C., Jones, C., Shen, Y., Clark, N. A., & Giesselmann, F. (2009). *Chem. Phys. Chem.*, *10*, 890.

[13] Andersson, G., Dahl, I., Keller, P., Kuczynski, W., Lagerwall, S. T., Skarp, K., & Stebler, B. (1987). *Appl. Phys. Lett.*, *51*, 640.

[14] Lagerwall, S. T., Rudquist, P., & Giesselmann, F. (2009). *Mol. Cryst. Liq. Cryst.*, *510*, 148.

[15] Bahr, C., & Heppke, G. (1987). *Mol. Cryst. Liq. Cryst.*, *150b*, 313; (1989). *Phys. Rev. A*, *39*, 5459; (1990). *Phys. Rev. A*, *41*, 4335.

[16] de Gennes, P. G., & Prost, J. (1993). *The Physics of Liquid Crystals* (2nd ed.), Clarendon Press: Oxford, 534.

[17] Walba, D., *et al.* (2007). *Journal of the SID*, *15/8*, 1.

[18] Walba, D., personal communication.

[19] Ostrovskij, B. I., Rabinovitch, A. Z., & Chigrinov, V. G. (1980). In: *Advances in Liquid Crystal Research and Applications*, Bata, L. (Ed.), Pergamon Press, Oxford/Akademiai Kiadó: Budapest, 469.

[20] Beresnev, L. A., Blinov, L. M., Dergachev, D. I., & Kondratjev, S. B. (1987). *JETP Lett*, *413*.

[21] Verhulst, A. G. H., Cnossen, G., Fünfschilling, J., & Schadt, M. (1994). *IDRC'94 Digest*, 377; Verhulst, A. G. H., & Cnossen, G. (1995). *IDW'95 Digest*, 35.

[22] Meyer, R. B. (1974). Presentation at the 5th ILCC Stockholm; Meyer, R. B., Liébert, L., Strzelecki, L., & Keller, P. (1975). *Le Journal de Physique*, *36*, L-69; Meyer, R. B. (1977). *Mol. Cryst. Liq. Cryst.*, *40*, 33.

[23] Carlsson, T., Osipov, & M. A. (1999). *Phys. Rev. E*, *60*, 5619. The field-induced rotational instabilities in chiral smectics were discovered by the Chalmers group and for the first time reported at the 13th ILCC in Vancouver in 1990 and then, in more detail, at the FLC conference in Tokyo 1993. The original results were never published as we had the ambition to present the experiments together with a valid theoretical interpretation but were unsuccessful to find one. Experiments were later taken up by Hope Ishi Erikson (Master Thesis Chalmers 1995), Lachezar Komitov, and in particular by Michel Mitov and Ingo Dierking. Later on Mikhail Osipov, then visiting professor at Chalmers, was able to find out the correct microscopic mechanism behind the effect.

[24] Michel Mitov (now at CEMES, Toulouse), unpublished work. Michel performed this work together with H. I. Erikson as visiting research fellow at Chalmers.

[25] Rieker, T. P., Clark, N. A., Smith, G. S., Parmar, D. S., Sirota, E. B., & Safinya, C. R. (1987). *Phys. Rev. Lett.*, *59*, 2658.

[26] Asao, Y., *et al.* (1999). *Jpn. J. Appl. Phys.*, *38*, 5977.

[27] Takezoe, H., Presentation O 26 at FLC'89; Galerne, Y. Presentation O 27 at FLC'89; Chandani, A. D. L., Gorecka, E., Ouchi, Y., Takezoe, H., & Fukuda, A. (1989). *Jpn. J. Appl. Phys.*, *28*, L1265; Galerne, Y., & Liébert, L. (1990). *Phys. Rev. Lett.*, *64*, 906.

[28] Qian, T., & Taylor, P. L. (1999). *Phys. Rev. E*, *60*, 2978; Wen, B., *et al.* (2000). *Phys. Rev. E*, *62*, 8152; Parry-Jones, L. A., & Elston, S. J. (2001). *Appl. Phys. Lett.*, *79*, 2097; Rudquist, *et al.* (2002). *Phys. Rev. E*, *66*, 061708.

[29] D'havé, K., *et al.* (2000). *Appl. Phys. Lett.*, *76*, 3528; D'havé, K., *et al.* (2000). *Ferroelectrics*, *244*, 115.

[30] Rudquist, P. (2005). Orthoconic antiferroelectric liquid crystals. In: *Chiral Liquid Crystals*, Kuczynski, W. (Ed.), Polish Academy of Sciences: Poznan.

[31] Levelut, A. M., *et al.* (1983). *Journal de Physique*, *44*, 623.

[32] Coles, H. J., *et al.* (1996). *U.K. Patent* GB2 317 186B; Kloess, P., *et al.* (1996). *Ferroelectrics*, *180*, 233; Robinson, W., *et al.* (1997). *Liq. Cryst.*, *23*, 309; Robinson, W. K., *et al.* (1998). *Liq. Cryst.*, *25*, 301; Carboni, C., *et al.* (1998). *Ferroelectrics*, *212*, 161; Lehmann, P., Robinson, W. K., & Coles, H. J. (1999). *Mol. Cryst. Liq. Cryst.*, *328*, 221; Carboni, C., & Coles, H. J. (1999). *Mol. Cryst. Liq. Cryst.*, *328*, 349.

[33] Lagerwall, S. T., *et al.* (2001). *Adv. Funct. Mater.*, *11*, 87.

[34] Taylor, T. R., Fergason, J. L., & Arora, S. L. (1970). *Phys. Rev. Lett.*, *24*, 359.

[35] De Meyere, A., Fornier, J., & Pauwels, H. (1996). *Ferroelectrics*, *181*, 1.

[36] Andersson, G., Dahl, I., Kuczynski, W., Lagerwall, S. T., Skarp, K., & Stebler, B. (1988). *Ferroelectrics*, *84*, 285.

[37] This was recently pointed out to me by Patrice Rannou at CNRS, CEA, Grenoble.

[38] Fujisawa, T., Hayashi, M., Hasebe, H., Takeuchi, K., Takatsu, H., & Kobayashi, S. (2007). *DIC Technical Review.*, *13*, 1–57.

[39] Mitsui, T. in LANDOLT-BÖRNSTEIN, "Ferroelectrics and Related Substances", Volume 28 (Supplement and Extention to Volume III/16 (1990), page 2.

[40] Lagerwall, S. T., Rudquist, P. G., & Herman, D. S. (2003). Liquid crystals – new electro-optic modes and applications. In: *Encyclopedia of Optical Engineering*, Marcel Dekker Inc.: New York, 1136–1150.

[41] Clark, N. A., & Lagerwall, S. T. (1980). *Appl. Phys. Lett.*, *36*, 899.